15 August 2019

Labeling proteins within *Drosophila* embryos by combining FRET reporters, position-specific genomic integration, and GAL4-reponsive expression <141>

Tzyy-Chyn Deng¶,[1] Chia-Jung Hsieh¶,[1] Michael De Freitas,[1] Maria Boulina,[1] Nima Sharifai,[1] Hasitha Samarajeewa,[1] Tatsumi Yanaba,[1] James D. Baker,[1] Michael D. Kim,[1] Susan Zusman,[2] Kenneth H. Wan,[3] Charles Yu,[3] Susan E. Celniker[3] and Akira Chiba[1]

[1]Department of Biology, University of Miami, Coral Gables, Florida 33146, USA, [2]Genetic Services Inc., Sudbury, MA 01776, USA, [3]Department of Genome Dynamics, Lawrence Berkeley National Laboratory, Berkeley, CA 94720, USA

¶ Contributed equally to this project.

Protein interaction network (PIN) or interactome has been mapped vigorously for the entire genome. We recognize, nonetheless, that such a map could illuminate profound insights had its context been revealed. We describe a scalable protein labeling method that could re-supply natural context back to the map of protein interactome. Genetically encoded fluorescent proteins, position-specific genomic integration and GAL4-responsive expression control enable labeling proteins *A, B* and *C* each with a either an eGFP, mCherry or NirFP in specified cells of optically transparent animals such as *Drosophila* embryos. While following multiple proteins through development and behavior, these labels offer separable pairs of Förster resonance energy transfer between proteins *A* and *B* and proteins *B* and *C*. We test and observe FRET interactions between specific protein pairs controlling cytoskeleton, nuclear signaling and cell polarity. By using our protein labeling method, it will be possible to map protein interaction network *in situ* — isPIN. <150>

(with 4 Tables and 6 Figures)

Key words: eGFP, mCherry, NirFP, FRET

Contributions: CH, TD, SC and AC conceived the project. CY, KW and SC designed and made the eGFP and mCherry expression vectors and expression clones. TD, MB and NS made NirFP expression clones. SZ and TD made transgene lines. TD and CH established stocks. CH, MD, TD, NS and HS performed microscopy, and TY, JD and MK assisted. AC with inputs from other co-authors wrote the paper.

Acknowledgements: We thank TK Harris and Rajeev Probhakar for structural biology of GFP, Konstantin Lukyanov for chemistry of NirFP, Edward Giniger, Francisco Raymo, and Peter Larsson for discussions on FRET-based protein imaging, Grace Zhai for discussion on *Drosophila,* Laura Bianchhi and Kevin Collins for discussion on *C. elegans*, Julia Dallman and Sandra Rieger for discussion on zebra fish, and Vance Lemmon, Patelis Tsoulfas and Tom Lisse for discussion on mice.

Supported in part by research awards RC2-NS069488 from American Recovery and Reinvestment Act and National Institutes of Health and MH079432 from National Institutes of Health to AC, and research award P41HG3487 from National Human Genome Research Institute to SC, and performed under U.S. Department of Energy Contracts DE-AC0376SF00098 and DE-AC02-05CH11231.

INTRODUCTION

Protein interaction network (PIN) or interactome has been mapped vigorously for the entire genome of *Drosophila* (Giot et al., 2003; Guruharsha et al., 2011) and human (Hein et al., 2015; Rolland et al., 2014). We recognize, nonetheless, that such a map could illuminate profound insights had its context been revealed. Since 1994, GFP (green fluorescent protein) (Chalfie et al., 1994) and other genetically encoded fluorescent proteins (Tsien, 1998) have labeled numerous proteins. They are useful in exposing inherent distribution biases of proteins within cells of diverse animals (Lukyanov, 2011), as well as serving as an immunological tag for purification of additional proteins capable of co-complexing (Guruharsha et al., 2011; Hein et al., 2015). In addition to these applications, valuable information regarding the way proteins interact *in vivo* can be collected using labeled proteins. Proximity attained by a pair of proteins that are labeled with spectrally overlapping fluorophores induces Förster resonance energy transfer (FRET)*, i.e.,* transfer of energy at near field from a fluorescence donor to a fluorescence acceptor (Förster, 1948). Therefore, occurrence of FRET as described best through quantum physics (Lakowicz, 2006) serves as a visual proxy for when and where proteins of interest interact with one another (Clegg, 2010). The idea of proximity-based scrutiny of interacting proteins (Sharifai et al., 2014) is not new, as the use of two-domain protein GAL4 transcription factor of yeast (Fields and Song, 1989) has expanded successfully to non-yeast proteins (Giot et al., 2003; Rolland et al., 2014). In contrast to yeast two-hybrid assays that sensitively demonstrate proteins' binding compatibility, we maintain the native environment of the proteins we assess although, similarly to these assays, for a pair at a time. Our optimization aims for both the quality design in labeling proteins and the tight control in expressing labeled proteins. By using our protein labeling method (see **Table1**), it will be possible to re-supply natural context back to the map of protein interactome.

RESULTS

To label individual proteins, we chose genetically encoded fluorescent proteins eGFP (Bierhuizen et al., 1997), mCherry (Shaner et al., 2004) and NirFP (Shcherbo et al., 2010) (**FIG1**). These labels serve as versatile imaging tools to study proteins within live animals. First, each of these fluorophores has structural resemblance to a "cage". This cage-like configuration is likely the strongest natural means for protecting a set of fluorescing atoms from surrounding stress. More specifically, the extremely rare ß sheet barrels constituting these proteins are proposed to solidly safeguard a small α helix, T65-Y66-G67 in eGFP for instance, capable of exhibiting fluorescent properties (Ormo et al., 1996). Another well-known example of ß sheet barrels protecting delicate internal structures occurs among channel proteins, such as in a tetrameric potassium channel (Zhou et al., 2001), that regulate ion selectivity of the cell surface. Second, each of these fluorescent labels is physically linked to a protein of interest through a "loop." Unlike synthetic chemicals that need conjugation through much weaker non-covalent bonds, this robustly covalent yet non-structural linkage achieves two consequences: (*1*) a short and constant distance between the label and the protein that is labeled, and (*2*) randomization of dipole orientation known as κ^2 of the label with respect to the protein it labels. Unlike synthetic fluorescent dyes (Pertz et al., 2006) or fluorescence-absorbing metal atoms (Koch and Larsson, 2005), neither eGFP, mCherry, nor NirFP requires pre-imaging dissection or incubation of animals after attaining full maturation, typically within 2-4 hours. As mentioned elsewhere (Chong et al., 2015; Hudson et al., 2008; Sarov et al., 2012; Trinh le et al., 2011; Venken et al., 2011), these and other genetically encoded fluorescent proteins are extremely valuable for time lapse imaging of proteins during development and behavior of animals. eGFP, mCherry and NirFP are derived from jellyfish *Aequoria* and sea anemone, *Discosoma* and *Entacmaea,*

respectively. Unlike their natural forms, however, custom-tuned eGFP and mCherry are each monomeric and do not dimerize by themselves. Also important, these two and NirFP do not bind one another directly when co-expressed in model organisms such as *Drosophila* (our observation). This is satisfactory because during imaging, both eGFP and mCherry are required to serve as a FRET donor**.** Any inherent affinity, whether previously known or unknown, between labeled proteins needs to be the sole reason for inducing FRET. Absorption and emission spectra of these fluorescent labels are distinct from each other. Notably, the eGFP-mCherry-NirFP trio offers two excellent yet separable FRET pairs: eGFP-to-mCherry with a Förster distance of 5.2 nm and mCherry-to-NirFP with a Förster distance of 4.4 nm. Multiplexing FRET capabilities using this trio may therefore serve as the basis for exposing the logic governing and/or the extent delimiting proteins interacting with each other (not shown). Although we are not aware of any systematic test on the functional neutrality of protein labeling, we believe that genetic knockouts of any specific proteins, if attempted, may be rescued by using fluorescently labeled but otherwise wild type forms of proteins. In fact, the very first use of GFP in fruit flies reported that genetic knockout of a certain nuclear protein could be rescued by expressing a GFP-fused wild-type form (Wang and Hazelrigg, 1994). More recently, Cdc42 protein, required for initiating the dendrites in neurons (Kamiyama and Chiba, 2009), was shown to rescue animals lacking a *cdc42* gene, regardless of whether the wild type transgene was fused to eGFP or not (our observation). We did not adopt split GFP as in the GRASP method (Feinberg et al., 2008) or sequential two-step GFP formation as in the GFP11 knock-in method (Kamiyama et al., 2016) because these strategies do not distinguish transient from permanent interactions. It should be further noted that these fluorescent proteins cannot readily fuse to DNA or RNA covalently, thus limiting their potential usage for exposing binding specificity of certain transcription factors or other DNA-binding/RNA-binding proteins toward particular nucleotide sequences through FRET.

We developed expression vectors, pUAS-C-eGFP-BD-attB, pUAS-C-mCherry-BD-attB, pUAS-N-eGFP-BD-attB and pUAS-N-mCherry-BD-attB for generating fluorescently tagged proteins of interest (POIs) (**FIG2**). First, we transferred protein open reading frames (ORFs) to the expression vectors using the Cre-Lox recombination cloning system, similar to the strategy used to make FLAG-HA constructs for tandem-affinity purification conducted previously (Guruharsha et al., 2011). The use of 100% sequence-validated XO and XS clone sets (Yu et al., 2011) prevents any unknown or non-intentional modification of the proteins being analysed. For 286 selected genes we used 283 BO clones to produce carboxyl terminal fusions from the XO clone set and 264 BS clones to produce amino terminal fusions from the XS clone set. We generated 953 expression clones in total: 236 UGS (eGFP amino tag), 245 URS (mCherry amino tag), 228 UGO (eGFP carboxyl tag) and 244 URO (mCherry carboxyl tag). Second, the *attp* sequence added to each expression vector is required for targeted integration of transgenes into specific landing sites in the *Drosophila* genome. We used phiC31 integrase, as originally characterized in retroviruses (Groth et al., 2004). The landing sites selected, *attp40* and *vk01* on chromosome 2 and *attp2* on chromosome 3, have high integration rates and are also known to induce sufficiently high rates of expression as GAL4-reponsive transgenes (Markstein et al., 2008; Venken et al., 2006a). It is also straightforward to introduce two transgenes onto one chromosome as a double transgene stock though intentional homologous recombination. Third, a tandem *UAS* sequence added to the vectors allows for expressing transgenes under the control of yeast GAL4 transcription factor (Brand and Perrimon, 1993). This enhancer hijacking in a foreign host genome*, i.e., Drosophila* in our case, offers total control over the time and place for co-expressing up to three transgenes all at a constant dosage.

Using this position-specific integration in the *Drosophila* genome, various single transgene, double transgene, and triple transgene stocks can be created (**FIG3***a-c*). Homologous

recombination occurs in the female germ line and, therefore, the use of balancer chromosomes during standard genetic crosses suppresses unwanted recombination of two transgenes in a single chromosome, *e.g.,* chromosome *ii*. As illustrated schematically, intentional uses of balancers afford stress-free combination of multiple transgenes, with all undergoing expression at constant dosage. Incidentally, a single genetic dosage is sufficient for detecting fluorescence from all labeled proteins, as well as detecting FRET quantitatively. The low-dosage expression also minimizes photo-toxicity during repeated and/or time-lapse imaging. The genotype of typical experimental animals has three GAL4-responsive transgenes for co-expressing proteins *A, B* and *C* labeled with eGFP, mCherry and NirFP, respectively, allowing for visualization of co-localizing POIs (**FIG3***d*). Similarly, when a protein couple is present, the two may exhibit specific affinity with each other and can be directly demonstrated through FRET (**FIG3***e*). Nevertheless, all FRET quantifications are to be compared to "*blank*" controls in which the fluorescently labeled POI is co-expressed with un-fused (cytoplasmic) fluorescent labels.

A label may be added to either the amino or carboxyl terminus of any POI, offering independent ways to visualize the same protein in the same microenvironment (**FIG4***a*). The same protein may be labeled by any of the three colors (**FIG4***b*). In our experience, choice in the label position or label color has not altered the intensity or distribution pattern of fluorescence, supporting their interchangeability as labels. The GAL4 driver may be ubiquitously expressed (*e.g., tub-GAL4* drives expression in all cells throughout development), specific to a whole tissue (*e.g., elav-GAL4* drives expression in all neuronal but not glia cells) or to a single cell (*e.g., eve*-GAL4 drives expression in aCC motoneurons in addition to frequent pCC interneurons and RP2 motoneurons in all 14 segments of the ventral nerve cord) (**FIG4***c*). In neuroscience, the question of presynaptic versus postsynaptic components of synapses is important as discussed on long-term potentiation, for example (Sanes and Lichtman, 1999). Being able to limit expression to either the presynaptic neurons, postsynaptic neurons or target cells would be valuable. In a general sense, biology of multi-compartmental cells can be scrutinized in ways not easily possible with endogenous or other non-GAL4 controls. The three fluorescent colors may label three different proteins *A, B* and *C* in the same cell or cell type defined by a particular GAL4 driver (**FIG5**). There, proteins may be observed in patterns that are unique to each tissue and/or a single cell within a given animal. Co-expression is necessary but not predictive of their interaction, nevertheless. In fact, patterns of expression for each protein as well as those of co-expression may not correlate at all to when and where FRET occurs (**FIG6**). Therefore, the true protein interactomic map awaits future characterization though direct imaging of fluorescently labeled proteins within animals, *i.e.,* the natural context.

DISCUSSION

The labeling method described in this paper employs the exogenous GAL4 system. Potential drawbacks of this, or any other methods not using the endogenous expression control, are two-fold. First, the timing and dosage of expression can be inappropriate for assessing the function of the protein of interest. The endogenous expression patterns are often available through mRNA *in situ* hybridization and/or antibody staining of their gene products. In theory, one can focus only on sites and times that are justifiable. Even so, any difference between the native endogenous expression and controlled exogenous expression can be a cause of concerns. Second, the endogenous gene expression remains untouched. Consequently, labeled protein *A* would potentially interact with both exogenously expressed and endogenously present labeled protein *B* and un-labeled protein *B*, respectively. When looking for evidence of FRET, there is always a possibility of under-estimating the true interaction probability between proteins *A* and *B*. (*Note:* Protein trapping, that in theory circumvent issues arising from endogenous versus

exogenous expression controls, has been designed for the *Drosophila* studies using green and red fluorescent proteins (Quinones-Coello et al., 2007; Venken et al., 2011); but the method described in this paper integrates notable advantages — see below.)

Our method incorporates several useful design concepts (see **Table 1**). In particular, the use of genetically encoded fluorescent proteins guarantees a one-to-one relationship between the label and the labeled. Also, their sturdy yet flexible linkers are thought to drastically simplify FRET computation. In addition, the GAL4 expression system, despite the discussion above, offers an unparalleled control over the time and place of expression, as well as maintaining it at a constantly low dosage. Furthermore, with position-specific transgene integration, the variability of transgene expression levels — a major source of complication in many genetic experiments — becomes minimal if not a non-issue in practice. As an added advantage, it is relatively straightforward to combine multiple labeled proteins through a series of genetic crosses. An additional detail not to be overlooked is that with an ever-expanding list of available GAL4 drivers (Jenett et al., 2012), the access to single cells becomes increasingly feasible. This would grant a significant advantage to neuroscience where axons, dendrites and synapses of the same cell can manifest distinct properties. Altogether, co-localization of three proteins *A, B* and *C,* as well as possible interaction between *A* and *B,* independent of the interaction between *B* and *C,* may all be documented. Finally, principles from most of these genetic engineering tools may be applicable to other metazoan model organisms such as nematodes, zebra fish and small mammals. Whether or not the concepts used in design of labeling or expression control may vary in detail, proteins that are labeled fluorescently in diverse animal systems will open a way to map freely interacting proteins within their natural context.

METHODS

Acceptor Vector construction. To generate the C-terminus tagged vectors, the pUAST expression vector (Brand and Perrimon, 1993) was cut with NotI and XbaI. The pUAST-C-TAP-BD expression vector (Stapleton) was cut with NotI and XbaI to release a 256 bp fragment containing loxP, chloramphenicol promoter and splice acceptor sequences. This 256 bp C-terminus BD cassette was inserted into the linearized pUAST vector by overnight ligation. The resulting C-terminus BD-adapted pUAST vector was linearized again by cutting it with XbaI. To generate the N-terminus tagged vectors, the pUAST expression vector was cut with EcoRI and XhoI. The pUAST-N-TAP-BD expression vector was cut with EcoRI and XhoI to release a 167 bp fragment containing loxP and chloramphenicol promoter sequences. This 167 bp C-terminus BD cassette was inserted into the linearized pUAST vector by overnight ligation. The resulting N-terminus BD-adapted pUAST vector was linearized again by cutting it with EcoRI. The CDS of the EGFP and mCherry fluorescent tags were obtained by PCR from the pEGFP-C1 (Clontech) and pRSET-B-mCherry (Invitrogen) vectors, respectively. C-terminus fluorescent tags were amplified using XbaI-tailed PCR primers, while N-terminus tags were amplified using EcoRI-tailed PCR primers (see below). The resulting PCR products were agrose gel-purified and cut with either XbaI (C-terminus tag) or EcoRI (N-terminus tag). Following ethanol precipitation, the XbaI digested C-terminus fluorescent tags were inserted into the XbaI linearized BD-adapted pUAST vector by overnight ligation. The EcoRI digested N-terminus tags were inserted into the EcoRI linearized BD-adapted pUAST vector by overnight ligation. The resulting C- or N-terminus fluorescent-tagged and BD-adapted pUAST vectors are cut with BamHI to release the portion of the vector containing the 5x UAS promoter, hsp70, BD cassette, fluorescent tag and SV40 terminator sequences. Agarose gel-purify the BamHI digested fragments. We linearized the pBDP vector by cutting it with BamHI and ethanol precipitated the digested product. We inserted the purified C- or N-terminus fluorescent-tagged and BD-adapted BamHI fragments

from the pUAST vectors into the linearized pBDP vector by overnight ligation. The resulting vectors are pUAS-C-EGFP-BD-attB, pUAS-C-mCherry-BD-attB, pUAS-N-EGFP-BD-attB and pUAS-N-mCherry-BD-attB. (*Note:* Expression vectors were designed similarly for labeling POI with NirFP but are yet unavailable at the DGRC.)

Sequences: 256bp C-terminus BD cassette: 5'-GGCCGCATAACTTCGTATAGCATACATTATACGAAGTTATAGATCCAATATTATTGAAGCATTTATCAGGGTTATTGTCTCATGAGCGGATACATATTTGAATGTATTTAGAAAAATAAACAAATAGGGGTTCCGCGCACATTTCCCCGAAAAGTGCCACCTGACGTGGATCTCGAGCTCAAGCTTCGAATTCAGGGTTTCCTTGACAATATCATACTTATCCTGTCCCTTTTTTTTCCACAGCTACCGGTCGCGT-3' 167bp N-terminus BD cassette: 5'-AATTCATAACTTCGTATAGCATACATTATACGAAGTTATAGATCCAATATTATTGAAGCATTTATCAGGGTTATTGTCTCATGAGCGGATACATATTTGAATGTATTTAGAAAAATAAACAAATAGGGGTTCCGCGCACATTTCCCCGAAAAGTGCCACCTGACGTC-3' XbaI-tailed PCR primers: C-mCherry-FWD 5'-cccctctagaGTGAGCAAGGGCGAGGAGGATAACATG-3' C-mCherry-REV 5'-ggggtctagaTTACTTGTACAGCTCGTCCATGCCGC-3' C-EGFP-FWD 5'-cccctctagaGTGAGCAAGGGCGAGGAGCTGTTC-3' C-EGFP-REV 5'-ggggtctagaTTACTTGTACAGCTCGTCCATGCCGAG-3' EcoRI-tailed PCR primers: mCherry-N-FWD 5'-ccccgaattcacaccATGGTGAGCAAGGGCGAGGAGGAT-3' mCherry-N-REV 5'-ggggaattcccCTTGTACAGCTCGTCCATGCCGCC-3' EGFP-N-FWD 5'-ccccgaattcacaccATGGTGAGCAAGGGCGAGGAGCTG-3' EGFP-N-REV 5'-ggggaattcccCTTGTACAGCTCGTCCATGCCGAG-3'

Expression Clone sets: We transferred ORFs from the BDGP *Drosophila melanogaster* XO and XS expression-ready clone sets to the pUAS-C-EGFP-BD-attB, pUAS-C-mCherry-BD-attB, pUAS-N-EGFP-BD-attB and pUAS-N-mCherry-BD-attB acceptor vectors (Yu et al., 2011). For recombination reactions, 200 ng of expression-ready Donor clone and acceptor Vector were recombined in a final volume of 10 µl for 15 minutes at 25 °C in a thermal cycler in the presence of Cre recombinase (0.2 units) and recombinase buffer supplemented with BSA (0.1 mg/ml) (Clontech #631614) according to Clontech manual PT3460-1 (now part of Takara Bio). Cre recombinase was inactivated by incubating the reaction at 70 °C for 10 minutes. From this reaction, 5 µl was transformed into chemically competent TAM-1 cells in a 96-well plate format (Active Motif #11096) and selected for Chloramphenicol resistance. Each clone was sequence verified to check for target mismatches using BigDye Terminator v3.1 ready reaction mix (Applied Biosystems #4337457) and the sequencing primer: 5'-GCCAATGTGCATCAGTTGTGGTC-3'. Sequencing samples were analyzed on a conventional capillary electrophoresis instrument (e.g., ABI 3730/3730xl DNA Analyzer). Glycerol stocks were generated and stored for each isolate. Clones can be obtained from the *Drosophila* Genome Resource Center (DGRC) in Bloomington, IN and sequence from GenBank using the accession numbers provided in Supplemental Table.

Drosophila *stocks. tub*-GAL4 - source: Bloomington Stock #60298 was used for ubiquitous expression. *elav*-GAL4 - source: Bloomington Stock # 8760 was used for pan-neuronal expression. *eve*-GAL4$^{[RN2\text{-GAL4-}E]}$ - source: M. Fuijoka was used for expression in aCC/RP2/pCC neurons. Transgenic flies carrying *UAS-eGFP::POI* (*attp40* site at 25C7 - source: www.geneticservices.com), *UAS-mCherry:POI* (*vk01* site at 59D3 - source: Bloomington Stock # 9722) on the second chromosome and *UAS-NirFP::POI* (*attp2* site at 68A4 - source: Bloomington Stock # 8622) on the third chromosome were constructed as described (Sharifai et al., 2014). All *attp* landing sites were selected because of their integration rates varying as high as 25-35%, *i.e.,* more efficiently than *P* element transformation of about 1%. *P Bac(y+.attp-3b) attp2* and *P Bac(y+.attp-3b) att40* are from the collections described in (Groth et al., 2004) and

(Szabad et al., 2012). They are located at map positions 25C6 (*attp40*) on the second chromosome and 68A4 (*attp2*) on the third chromosome. *PBac(y+.attp-3b) vk01* is from the Venken Bac collection (Venken et al., 2006b) and is located at 59D3 of the second chromosome. Besides their high integration rates, these integration sites were used also for high expression rates and low background effects (Markstein et al., 2008; Pfeiffer et al., 2010) (Zusman et al. unpublished observations). For all integration sites the integrase-producing transgene *P(nos-phiC31\int.NLS) X* (Bischof et al., 2007) was used.

Imaging. UAS-transgene carrying males were crossed with GAL4 driver carrying virgin females in mating cages using grape juice agar plates coated with yeast to collect embryos. Mating cages were placed at 25 °C and collection plates were swapped after one hour to gather embryos for a given developmental stage. Embryos were manually dechorionated and developmental staging was confirmed by gut morphology. Embryos were placed on double-sided tape attached to a glass slide with a silicone well and then immersed in HL3.1 hemolymph buffer for imaging. We used an upright microscope with a x40 or x63 water-immersion objective lens to image the sample. However, when an inverted microscope was used, a coverslip was placed over the buffer-immersed embryos using elastic silicone. Subsequently, the slide was flipped upside-down and mounted on a x40 or x63 oil-immersion objective lens. In some cases, devitillenization, filet dissection, or both, were performed to increase signal intensities of eGFP, mCherry and NirFP. A ratio of mCherry over eGFP being between 0.1 and 10 was found essential for obtaining reliable FRET measurements, consistent with previous findings (Berney and Danuser, 2003). No samples created through our transgenic method produced a sign of "false positive" FRET, *i.e.,* a false decrease in donor fluorescence lifetime. In contrast, experiments using standard retrovirus transfection methods in human and insect cell lines had an expression level of mCherry, the FRET acceptor, beyond the ratio of 100 and produced such a "false positive" FRET (not shown).

FRET probability. The probability of FRET is defined as a product of the concentration and lifetime reduction of a FRET donor, *e.g.,* eGFP or mCherry. Whereas the concentration of a given protein varies from pixel to pixel, the fluorescence lifetime τ is calculated independently of its concentration. Consequently, a polar histogram allows for normalization of the FRET probability irrespective of the size of proteins interacting with each other. This size-free unit of protein interactome is termed "interaction" (Sharifai et al., 2014).

REFERENCES

Berney, C., and Danuser, G. (2003). FRET or no FRET: a quantitative comparison. Biophys J *84*, 3992-4010.

Bierhuizen, M.F., Westerman, Y., Visser, T.P., Wognum, A.W., and Wagemaker, G. (1997). Green fluorescent protein variants as markers of retroviral-mediated gene transfer in primary hematopoietic cells and cell lines. Biochem Biophys Res Commun *234*, 371-375.

Bischof, J., Maeda, R.K., Hediger, M., Karch, F., and Basler, K. (2007). An optimized transgenesis system for Drosophila using germ-line-specific phiC31 integrases. Proc Natl Acad Sci U S A *104*, 3312-3317.

Brand, A.H., and Perrimon, N. (1993). Targeted gene expression as a means of altering cell fates and generating dominant phenotypes. Development *118*, 401-415.

Chalfie, M., Tu, Y., Euskirchen, G., Ward, W.W., and Prasher, D.C. (1994). Green fluorescent protein as a marker for gene expression. Science *263*, 802-805.

Chong, Y.T., Koh, J.L., Friesen, H., Duffy, S.K., Cox, M.J., Moses, A., Moffat, J., Boone, C., and Andrews, B.J. (2015). Yeast proteome dynamics from single cell imaging and automated analysis. Cell *161*, 1413-1424.

Clegg, R.M. (2010). Fluorescence lifetime-resolved imaging: what, why, how - a prologue. In FLIM microscopy in biology and medicine, A. Periasamy, and R.M. Clegg, eds., pp. 3-29.

Feinberg, E.H., Vanhoven, M.K., Bendesky, A., Wang, G., Fetter, R.D., Shen, K., and Bargmann, C.I. (2008). GFP Reconstitution Across Synaptic Partners (GRASP) defines cell contacts and synapses in living nervous systems. Neuron *57*, 353-363.

Fields, S., and Song, O. (1989). A novel genetic system to detect protein-protein interactions. Nature *340*, 245-246.

Förster, T. (1948). Intermolecular energy migration and fluorescence. Annalen der Physik *437*, 55-75.

Giot, L., Bader, J.S., Brouwer, C., Chaudhuri, A., Kuang, B., Li, Y., Hao, Y.L., Ooi, C.E., Godwin, B., Vitols, E.*, et al.* (2003). A protein interaction map of *Drosophila melanogaster*. Science *302*, 1727-1736.

Groth, A.C., Fish, M., Nusse, R., and Calos, M.P. (2004). Construction of transgenic Drosophila by using the site-specific integrase from phage phiC31. Genetics *166*, 1775-1782.

Guruharsha, K.G., Rual, J.F., Zhai, B., Mintseris, J., Vaidya, P., Vaidya, N., Beekman, C., Wong, C., Rhee, D.Y., Cenaj, O.*, et al.* (2011). A protein complex network of *Drosophila melanogaster*. Cell *147*, 690-703.

Hein, M.Y., Hubner, N.C., Poser, I., Cox, J., Nagaraj, N., Toyoda, Y., Gak, I.A., Weisswange, I., Mansfeld, J., Buchholz, F.*, et al.* (2015). A human interactome in three quantitative dimensions organized by stoichiometries and abundances. Cell *163*, 712-723.

Hudson, A.M., Petrella, L.N., Tanaka, A.J., and Cooley, L. (2008). Mononuclear muscle cells in *Drosophila* ovaries revealed by GFP protein traps. Dev Biol *314*, 329-340.

Jenett, A., Rubin, G.M., Ngo, T.T., Shepherd, D., Murphy, C., Dionne, H., Pfeiffer, B.D., Cavallaro, A., Hall, D., Jeter, J.*, et al.* (2012). A GAL4-driver line resource for Drosophila neurobiology. Cell reports *2*, 991-1001.

Kamiyama, D., and Chiba, A. (2009). Endogenous activation patterns of Cdc42 GTPase within *Drosophila* embryos. Science *324*, 1338-1340.

Kamiyama, D., Sekine, S., Barsi-Rhyne, B., Hu, J., Chen, B., Gilbert, L.A., Ishikawa, H., Leonetti, M.D., Marshall, W.F., Weissman, J.S.*, et al.* (2016). Versatile protein tagging in cells with split fluorescent protein. Nature communications *7*, 11046.

Koch, H.P., and Larsson, H.P. (2005). Small-scale molecular motions accomplish glutamate uptake in human glutamate transporters. J Neurosci *25*, 1730-1736.

Lakowicz, J.R. (2006). Protein Fluorescence (Springer Science & Business Media).

Lukyanov, K.A. (2011). Green-red flashers to accelerate biology. Chem Biol *18*, 1202-1204.

Markstein, M., Pitsouli, C., Villalta, C., Celniker, S.E., and Perrimon, N. (2008). Exploiting position effects and the gypsy retrovirus insulator to engineer precisely expressed transgenes. Nat Genet *40*, 476-483.

Ormo, M., Cubitt, A.B., Kallio, K., Gross, L.A., Tsien, R.Y., and Remington, S.J. (1996). Crystal structure of the Aequorea victoria green fluorescent protein. Science *273*, 1392-1395.

Pertz, O., Hodgson, L., Klemke, R.L., and Hahn, K.M. (2006). Spatiotemporal dynamics of RhoA activity in migrating cells. Nature *440*, 1069-1072.

Pfeiffer, B.D., Ngo, T.T., Hibbard, K.L., Murphy, C., Jenett, A., Truman, J.W., and Rubin, G.M. (2010). Refinement of tools for targeted gene expression in Drosophila. Genetics *186*, 735-755.

Quinones-Coello, A.T., Petrella, L.N., Ayers, K., Melillo, A., Mazzalupo, S., Hudson, A.M., Wang, S., Castiblanco, C., Buszczak, M., Hoskins, R.A.*, et al.* (2007). Exploring strategies for protein trapping in Drosophila. Genetics *175*, 1089-1104.

Rolland, T., Tasan, M., Charloteaux, B., Pevzner, S.J., Zhong, Q., Sahni, N., Yi, S., Lemmens, I., Fontanillo, C., Mosca, R.*, et al.* (2014). A proteome-scale map of the human interactome network. Cell *159*, 1212-1226.

Sanes, J.R., and Lichtman, J.W. (1999). Can molecules explain long-term potentiation? Nat Neurosci *2*, 597-604.

Sarov, M., Murray, J.I., Schanze, K., Pozniakovski, A., Niu, W., Angermann, K., Hasse, S., Rupprecht, M., Vinis, E., Tinney, M.*, et al.* (2012). A genome-scale resource for *in vivo* tag-based protein function exploration in *C. elegans*. Cell *150*, 855-866.

Shaner, N.C., Campbell, R.E., Steinbach, P.A., Giepmans, B.N., Palmer, A.E., and Tsien, R.Y. (2004). Improved monomeric red, orange and yellow fluorescent proteins derived from Discosoma sp. red fluorescent protein. Nat Biotechnol *22*, 1567-1572.

Sharifai, N., Samarajeewa, H., Kamiyama, D., Deng, T.C., Boulina, M., and Chiba, A. (2014). Imaging dynamic molecular signaling by the Cdc42 GTPase within the developing CNS. PLoS One *9*, e88870.

Shcherbo, D., Shemiakina, II, Ryabova, A.V., Luker, K.E., Schmidt, B.T., Souslova, E.A., Gorodnicheva, T.V., Strukova, L., Shidlovskiy, K.M., Britanova, O.V.*, et al.* (2010). Near-infrared fluorescent proteins. Nat Methods *7*, 827-829.

Szabad, J., Bellen, H.J., and Venken, K.J. (2012). An assay to detect in vivo Y chromosome loss in Drosophila wing disc cells. G3 *2*, 1095-1102.

Trinh le, A., Hochgreb, T., Graham, M., Wu, D., Ruf-Zamojski, F., Jayasena, C.S., Saxena, A., Hawk, R., Gonzalez-Serricchio, A., Dixson, A.*, et al.* (2011). A versatile gene trap to visualize and interrogate the function of the vertebrate proteome. Genes Dev *25*, 2306-2320.

Tsien, R.Y. (1998). The green fluorescent protein. Annu Rev Biochem *67*, 509-544.

Venken, K., De Gendt, K., Boonen, S., Ophoff, J., Bouillon, R., Swinnen, J.V., Verhoeven, G., and Vanderschueren, D. (2006a). Relative impact of androgen and estrogen receptor activation in the effects of androgens on trabecular and cortical bone in growing male mice: a study in the androgen receptor knockout mouse model. Journal of bone and mineral research : the official journal of the American Society for Bone and Mineral Research *21*, 576-585.

Venken, K.J., He, Y., Hoskins, R.A., and Bellen, H.J. (2006b). P[acman]: a BAC transgenic platform for targeted insertion of large DNA fragments in D. melanogaster. Science *314*, 1747-1751.

Venken, K.J., Schulze, K.L., Haelterman, N.A., Pan, H., He, Y., Evans-Holm, M., Carlson, J.W., Levis, R.W., Spradling, A.C., Hoskins, R.A.*, et al.* (2011). MiMIC: a highly versatile transposon insertion resource for engineering Drosophila melanogaster genes. Nat Methods *8*, 737-743.

Wang, S., and Hazelrigg, T. (1994). Implications for bcd mRNA localization from spatial distribution of exu protein in *Drosophila* oogenesis. Nature *369*, 400-403.

Yu, C., Wan, K.H., Hammonds, A.S., Stapleton, M., Carlson, J.W., and Celniker, S.E. (2011). Development of expression-ready constructs for generation of proteomic libraries. Methods Mol Biol *723*, 257-272.

Zhou, Y., Morais-Cabral, J.H., Kaufman, A., and MacKinnon, R. (2001). Chemistry of ion coordination and hydration revealed by a K+ channel-Fab complex at 2.0 A resolution. Nature *414*, 43-48.

Table 1. Tools for charting freely interacting proteins within live animals.[‡]

Tools	How	Why	Note
(*a*) Genetically-encoded fluorescent proteins.	Fuse protein of interest (POI) to eGFP, mCherry or NirFP.	Visualize co-localization of proteins, and detect possible interaction between them by FRET.	Structural features of the ß-barrel "cage" and flexible "loop" make eGFP, mCherry and NirFP reliable labels.
(*b)* Position-specific integration of transgene by PhiC31 integrase.	*attp* sequences allows integration of eGFP-labeled constructs to the *attp40* site and mCherry-labeled constructs to the *VK01* site on chromosome 2, and the NirFP-labeled constructs to the *attp2* site on chromosome 3.	Construct single, double and triple transgenic stocks through standard genetic crosses.	Landing sites selected are likely to be least problematic in terms of expressing labeled proteins.
(*c*) Expression control by GAL4 transcription factor.	Tandem *UAS* sequence allows for expressing transgenes under the control of a *GAL4* driver.	Control the time, place and dosage of expressing labeled proteins.	GAL4-resposive expressions typically cause no anatomical or behavioral anomalies.

[‡] We integrate: (*a*) genetically encoded fluorescent proteins, (*b*) PhiC31 mediated genomic integration and (*c*) GAL4 responsive expression control. Use of these tools is not technically limited to *Drosophila*.

Table 2. *Drosophila* cDNA. §

Gene	Gene Name	cDNA (Gold Source Clone)	nG (eGFP::ORF)	nR (mCherry::ORF)	cG (ORF::eGFP)	cR (ORF::mCherry)	4-way	2-way	FRET
Act42A	Actin 42A	LD18090	UGS01407	URS01407	UGO01207	URO01207	yes	yes	
Act5C	Actin 5C	RE02927	UGS01271	URS01271	UGO01171	URO01171	yes	yes	
Actn	alpha actinin	LD37956			UGO01162				
AdenoK	Adenosine Kinase	GH14845	UGS01220	URS01220		URO01120		yes	
ago	archipelago	LD21322	UGS01492	URS01492	UGO01292	URO01292	yes	yes	
Agpat1	1-Acylglycerol-3-phosphate O-acyltransferase 1	LD44987	UGS01215		UGO01322	URO01115		yes	
ALiX	ALG-2 interacting protein X	LD25543			UGO01331				
alph	alphabet	LD23542	UGS01372	URS01372		URO01072		yes	
amon	amontillado	GH12584			UGO01167	URO01167		yes	
AnxB9	Annexin B9	LD09947	UGS01331	URS01331	UGO01031	URO01031	yes	yes	

§ Proteins encoded by 288 sequence-validated Gold Source Clone cDNAs are each fused to either green eGFP (*G*) or red mCherry (*R*) at their amino terminus (*a*) or carboxyl terminus (*c*) (**FIG3**). Success rate for producing the transgenes in *E. coli* plasmids as *4-way* tagging, *i.e., cG, cR, nG* and *nR,* varied but on average was 83% (varying from 80-86% for each of the four sets); however, if one was to lower the expectation to *2-way* tagging of at least one eGFP and one mCherry, regardless of their tag position for each ORF, then the success rate rose in nearly all attempts (97%). *Asterisks* (★) indicate the biochemically demonstrated protein-protein binding compatibility that are anticipated to cause FRET between protein pairs, *e.g.,* Cdc42-to-WASp, Cdc42-to-Par6, Cdc42-to-RhoGAP, and WASp-to-Arp3 (see **Table4**). (*Note:* To request any of these 953 expression clones from Berkeley *Drosophila* Genome Project at **www.fruitfly.org**, both the cDNA accession number and their tag-specific expression clone number are required. **Supplementary Table** supplies a full-size Excel table of *Drosophila* cDNA.)

APC10	Anaphase Promoting Complex subunit 10	RE25242	UGS01487	URS01487	UGO01287	URO01287	yes	yes	
Aplip1	APP-like protein interacting protein 1	GH14842	UGS01385	URS01385		URO01085		yes	
Aplip1	APP-like protein interacting protein 1	RH26053	UGS01415		UGO01215	URO01215		yes	
Appl	beta amyloid protein precursor-like	GH04413			UGO01244	URO01244		yes	
Arf51F	ADP ribosylation factor at 51F	RE16882			UGO01177	URO01177		yes	
Arf79F	ADP ribosylation factor at 79F	LD24904	UGS01351	URS01351	UGO01051	URO01051	yes	yes	
ArfGAP3	ADP-ribosylation factor GTPase activating protein 3	LD46935	UGS01257	URS01257				yes	
Arp2	Actin-related protein 2	LD18955	UGS01357	URS01357		URO01057		yes	
Arp3	Actin-related protein 3	LD35711	UGS01204	URS01204	UGO01104			yes	★
Arpc2	Actin-related protein 2/3 complex, subunit 2	LD29815	UGS01202	URS01202	UGO01102	URO01102	yes	yes	
Arpc3B	Actin-related protein 2/3 complex, subunit 3B	SD24339	UGS01472	URS01472	UGO01272	URO01272	yes	yes	
Arpc5	Actin-related protein 2/3 complex, subunit 5	RH48239	UGS01256	URS01256		URO01156		yes	
Ate1	Arginyltransferase 1	LD23642	UGS01423	URS01423	UGO01223	URO01223	yes	yes	
Ate1	Arginyltransferase 1	LD33682	UGS01435	URS01435	UGO01235	URO01235	yes	yes	
Atg8a	Autophagy-related 8a	LD05816	UGS01328	URS01328		URO01028		yes	
ATPsynB	ATP synthase, subunit B	RE36486	UGS01478	URS01478	UGO01278	URO01278	yes	yes	
ATPsynbeta	ATP synthase, beta subunit	RE10864	UGS01430	URS01430	UGO01230	URO01230	yes	yes	
ATPsynd	ATP synthase, delta subunit	RE24457	UGS01463	URS01463	UGO01263	URO01263	yes	yes	

elta								
ATPsynG	ATP synthase, subunit G	RE20862	UGS01279	URS01279	UGO01179			yes
ATPsynga mma	ATP synthase, gamma subunit	RE35715	UGS01282	URS01282	UGO01182	URO01182	yes	yes
ATPsynO	ATP synthase, oligomycin sensitivity conferring protein	GH01760	UGS01378	URS01378	UGO01078	URO01078	yes	yes
ball	ballchen	LD09009	UGS01237	URS01237	UGO01137	URO01336	yes	yes
betaTub56D	beta-Tubulin at 56D	LD43681	UGS01406	URS01406		URO01206		yes
betaTub85D	beta-Tubulin at 85D	GH02051	UGS01404		UGO01204	URO01204		yes
blw	bellwether	HL08087	UGS01228	URS01228	UGO01128	URO01128	yes	yes
boi	brother of ihog	RE01910	UGS01269	URS01269	UGO01169	URO01169	yes	yes
bru1	bruno 1	LD29068	UGS01247	URS01247	UGO01147	URO01147	yes	yes
bs	blistered	RE17834	UGS01315	URS01315	UGO01015	URO01306	yes	yes
bsk	basket	HL02677	UGS01339	URS01339	UGO01309			yes
Btk29A	Btk family kinase at 29A	LD16208		URS01443	UGO01243			yes
Buffy	Buffy	AT16536	UGS01295	URS01295		URO01195		yes
cact	cactus	LD10168	UGS01317	URS01317		URO01017		yes
CanA1	Calcineurin A1	RE54552	UGS01468	URS01468	UGO01268			yes
CCT6	Chaperonin containing TCP1 subunit 6	GH13725	UGS01242	URS01242	UGO01142	URO01142	yes	yes
Cdc23	Cell division cycle 23	LD09850		URS01442	UGO01242	URO01242		yes
Cdc27	Cell division cycle 27	LD12661	UGS01473	URS01473	UGO01273			yes

Cdc42	Cell division cycle 42	HL08128			UGO01134	URO01134		yes	★
CDC45L	CDC45L	LD35753	UGS01251	URS01251	UGO01151	URO01151	yes	yes	
Cdk1	Cyclin-dependent kinase 1	LD38718	UGS01365	URS01365		URO01065		yes	
CG10077	-	GH10652			UGO01252	URO01252		yes	
CG10298	-	GH28351	UGS01471	URS01471		URO01271		yes	
CG11583	-	LD22010	UGS01350	URS01350	UGO01050	URO01050	yes	yes	
CG11807	-	SD03973	UGS01219	URS01219	UGO01119	URO01119	yes	yes	
CG13887	-	LP10861	UGS01360	URS01360	UGO01060	URO01060	yes	yes	
CG17739	-	GH02025	UGS01243	URS01243	UGO01143	URO01143	yes	yes	
CG1909	-	GH22690	UGS01246	URS01246		URO01146		yes	
CG2862	-	RH49748	UGS01292	URS01292	UGO01335	URO01192	yes	yes	
CG3008	-	RE33807	UGS01464		UGO01264	URO01264		yes	
CG31457	-	LD10183	UGS01332	URS01332	UGO01032	URO01032	yes	yes	
CG32137	-	RE18568	UGS01462	URS01462	UGO01262	URO01262	yes	yes	
CG3529	-	GH05942	UGS01382	URS01382	UGO01082	URO01082	yes	yes	
CG3788	-	AT31332	UGS01401	URS01401	UGO01201			yes	
CG42540	-	RE02540	UGS01434	URS01434	UGO01234	URO01234	yes	yes	
CG7220	-	AT19555	UGS01403	URS01403	UGO01203	URO01203	yes	yes	
CG8199	-	GH19141	UGS01388	URS01388	UGO01088	URO01088	yes	yes	
CG9281	-	LD02975	UGS01239	URS01239	UGO01139	URO01139	yes	yes	
Chc	Clathrin heavy chain	LD43101	UGS01486	URS01486				yes	

cin	cinnamon	GH09380			UGO01250	URO01250		yes
Cka	Connector of kinase to AP-1	LD41760			UGO01163	URO01163		yes
CkIIbeta	Casein kinase II beta subunit	RE31047	UGS01281	URS01281	UGO01181	URO01342	yes	yes
Cortactin	Cortactin	LD29964	UGS01248	URS01248		URO01148		yes
COX4L	Cytochrome c oxidase subunit 4-like	AT07685	UGS01293	URS01293	UGO01193	URO01193	yes	yes
Crk	Crk oncogene	RE60886		URS01418	UGO01218	URO01218		yes
csul	capsuleen	LD07634	UGS01408	URS01408	UGO01208	URO01208	yes	yes
csw	corkscrew	LD22829	UGS01235	URS01235	UGO01135	URO01135	yes	yes
CtsB1	Cathepsin B1	GH06546	UGS01383	URS01383		URO01083		yes
CycA	Cyclin A	LD44443	UGS01212	URS01212	UGO01112			yes
CycC	Cyclin C	LD35705	UGS01358	URS01358	UGO01311	URO01058	yes	yes
CycD	Cyclin D	LD22957		URS01371		URO01071		
CycG	Cyclin G	LD46284		URS01429	UGO01229			yes
Diap2	Death-associated inhibitor of apoptosis 2	LD34777		URS01203	UGO01103			yes
dj-1β	#N/A	GH09983	UGS01362		UGO01062	URO01062		yes
dnr1	defense repressor 1	LD18186		URS01441	UGO01241	URO01241		yes
dock	dreadlocks	LD42588	UGS01209	URS01209	UGO01109	URO01109	yes	yes
drk	downstream of receptor kinase	LD12029	UGS01238	URS01238	UGO01138	URO01138	yes	yes
Dsor1	Downstream of raf1	LD41207	UGS01252		UGO01152	URO01152		yes
Dsp1	Dorsal switch protein 1	GM02110	UGS01341	URS01341	UGO01041	URO01314	yes	yes

E(z)	Enhancer of zeste	LD30505	UGS01322	URS01322		URO01022		yes
Eaat2	Excitatory amino acid transporter 2	GH09856*	UGS01421	URS01421	UGO01221	URO01221	yes	yes
eIF4B	eukaryotic translation initiation factor 4B	RE54950	UGS01326	URS01326	UGO01026	URO01310	yes	yes
eIF4E1	eukaryotic translation initiation factor 4E1	RE36735	UGS01417	URS01417	UGO01217	URO01217	yes	yes
Ent1	Equilibrative nucleoside transporter 1	LD19162	UGS01333	URS01333		URO01033		yes
exd	extradenticle	LD03509	UGS01305	URS01305	UGO01005	URO01005	yes	yes
FeCH	Ferrochelatase	GH01314	UGS01377	URS01377	UGO01317	URO01324	yes	yes
FeCH	Ferrochelatase	SD11336	UGS01426	URS01426	UGO01226			yes
Flo1	Flotillin 1	SD10657		URS01447	UGO01247	URO01247		yes
Flo2	Flotillin 2	LP11503	UGS01223	URS01223	UGO01123			yes
Flo2	Flotillin 2	RE74011		URS01431	UGO01231			yes
flw	flapwing	GH05039		URS01494	UGO01294	URO01294		yes
Fnta	Farnesyl transferase alpha	LD26412	UGS01366	URS01366	UGO01312	URO01066	yes	yes
fzr	fizzy-related	GH07620	UGS01411	URS01411	UGO01211	URO01211	yes	yes
Gad1	Glutamic acid decarboxylase 1	HL02049	UGS01344	URS01344		URO01044		yes
Galphai	G protein alpha i subunit	LD22201	UGS01370	URS01370	UGO01070	URO01320	yes	yes
Galphao	G protein alpha o subunit	GM01620		URS01340	UGO01040	URO01040		yes
Galphas	G protein alpha s subunit	LD26182		URS01229	UGO01129	URO01129		yes
gammaCOP	Coat Protein (coatomer) gamma	RE37840	UGS01233	URS01233	UGO01326			yes

Gbeta13F	G protein beta-subunit 13F	LD25526	UGS01394		UGO01094	URO01094		yes
Gbeta5	Gbeta5	RH17413	UGS01289	URS01289	UGO01189	URO01344	yes	yes
Gdi	GDP dissociation inhibitor	LP03430			UGO01012	URO01305		yes
GMF	Glia maturation factor	RE40543	UGS01477	URS01477	UGO01277	URO01277	yes	yes
Gp93	Glycoprotein 93	LD23641	UGS01485	URS01485		URO01285		yes
grn	grain	RE40104	UGS01309	URS01309		URO01303		yes
gsb-n	gooseberry-neuro	RE64348	UGS01321	URS01321		URO01021		yes
gus	gustavus	LD34464	UGS01224	URS01224	UGO01124	URO01124	yes	yes
Gyg	Glycogenin	RE02181	UGS01270	URS01270	UGO01170	URO01170	yes	yes
h	hairy	RE40955	UGS01303	URS01303	UGO01003	URO01003	yes	yes
HDAC1	Histone deacetylase 1	GM14158	UGS01368	URS01368	UGO01068	URO01068	yes	yes
HDAC3	Histone deacetylase 3	LD23745	UGS01373	URS01373		URO01321		yes
HDAC6	Histone deacetylase 6	LD43531	UGS01455	URS01455	UGO01255			yes
Hex-C	Hexokinase C	RH33703	UGS01291	URS01291	UGO01191			yes
Hmgs	HMG Coenzyme A synthase	LD26976	UGS01201	URS01201	UGO01101	URO01101	yes	yes
Hnf4	Hepatocyte nuclear factor 4	RE09535		URS01311	UGO01011	URO01011		yes
Hpd	4-hydroxyphenylpyruvate dioxygenase	GH03058	UGS01386	URS01386	UGO01086	URO01326	yes	yes
Hpd	4-hydroxyphenylpyruvate dioxygenase	GH11957	UGS01419	URS01419	UGO01219	URO01219	yes	yes
Hr96	Hormone receptor-like in 96	GH14435	UGS01319	URS01319		URO01309		yes
Hrb87F	Heterogeneous nuclear ribonucleoprotein at 87F	LD32727	UGS01420	URS01420	UGO01220	URO01220	yes	yes

HtrA2	HTRA2-related serine protease	AT14262	UGS01294	URS01294	UGO01194	URO01194	yes	yes
I-2	Inhibitor-2	LD47783	UGS01493	URS01493	UGO01293	URO01293	yes	yes
ICA69	Islet cell autoantigen 69 kDa	GH23156	UGS01389	URS01389	UGO01089			yes
Ilk	Integrin linked kinase	LD24671	UGS01375	URS01375	UGO01316	URO01323	yes	yes
Imp	IGF-II mRNA-binding protein	SD07045				URO01258		
Jra	Jun-related antigen	LD25202	UGS01302	URS01302		URO01002		yes
Klp61F	Kinesin-like protein at 61F	LD15641	UGS01440	URS01440	UGO01240	URO01240	yes	yes
krz	kurtz	LD31082	UGS01439	URS01439	UGO01239			yes
LamC	Lamin C	LD31805	UGS01250	URS01250	UGO01150	URO01150	yes	yes
lid	little imaginal discs	LD40310			UGO01304	URO01025		yes
Liprin-alpha	Liprin-alpha	LD33094			UGO01161	URO01338		yes
Lis-1	Lissencephaly-1	LD11219	UGS01409	URS01409	UGO01209	URO01209	yes	yes
Lmpt	Limpet	RE22626	UGS01482	URS01482	UGO01282			yes
loqs	loquacious	RE14437	UGS01275	URS01275	UGO01332	URO01175	yes	yes
Mad	Mothers against dpp	RE72705	UGS01316	URS01316		URO01307		yes
Mbs	Myosin binding subunit	GH16214	UGS01445	URS01445	UGO01245			yes
metro	menage a trois	GH12103	UGS01448	URS01448	UGO01248	URO01248	yes	yes
mew	multiple edematous wings	GH14509	UGS01258	URS01258	UGO01330	URO01158	yes	yes
Mkk4	MAP kinase kinase 4	RE70055	UGS01232	URS01232		URO01132		yes
MRG15	MORF-related gene 15	LD22902	UGS01393	URS01393	UGO01093	URO01093	yes	yes

mRpL40	mitochondrial ribosomal protein L40	RE65766	UGS01287	URS01287	UGO01334	URO01187	yes	yes	
mts	microtubule star	LD26077	UGS01396	URS01396		URO01096		yes	
mys	myospheroid	RE55238	UGS01488	URS01488	UGO01288	URO01288	yes	yes	
Nedd4	Nedd4	SD04682			UGO01165	URO01165		yes	
Nf-YA	Nuclear factor Y-box A	LD21748		URS01307	UGO01007	URO01007		yes	
Nf-YC	Nuclear factor Y-box C	RE43755	UGS01310	URS01310	UGO01022	URO01304	yes	yes	
Nmt	N-myristoyl transferase	GM13220		URS01345	UGO01045	URO01315		yes	
nSyb	neuronal Synaptobrevin	GH04664		URS01354	UGO01054	URO01054		yes	
nudE	nudE	LD19982	UGS01334	URS01334	UGO01034	URO01034	yes	yes	
Oat	Ornithine aminotransferase precursor	GH01984	UGS01379	URS01379		URO01079		yes	
Osbp	Oxysterol binding protein	LD31802			UGO01160	URO01160		yes	
p130CAS	p130CAS	GH02705	UGS01244	URS01244	UGO01144	URO01144	yes	yes	
p38b	p38b MAP kinase	LD24658	UGS01241	URS01241	UGO01141	URO01141	yes	yes	
p53	p53	GH11591	UGS01306	URS01306	UGO01006	URO01006	yes	yes	
p53	p53	AT28346	UGS01402	URS01402	UGO01202	URO01202	yes	yes	
Pak3	Pak3	LD10376	UGS01489		UGO01289	URO01289		yes	
par-6	par-6	LD29223	UGS01227	URS01227	UGO01325	URO01127	yes	yes	★
Parp	Poly-(ADP-ribose) polymerase	RE04933	UGS01481	URS01481	UGO01281			yes	
parvin	parvin	GH23568	UGS01422	URS01422	UGO01222	URO01222	yes	yes	
Pde1c	Phosphodiesterase 1c	RE56844			UGO01266				
Pdk1	Phosphoinositide-dependent kinase 1	LD22131			UGO01253	URO01253		yes	

Pdp1	PAR-domain protein 1	GM02880			UGO01001	URO01301		yes
Pect	Phosphoethanolamine cytidylyltransferase	RE62261	UGS01416	URS01416	UGO01216			yes
Pepck2	Phosphoenolpyruvate carboxykinase 2	RE12569	UGS01460	URS01460	UGO01260	URO01260	yes	yes
Pex13	Peroxin 13	RE69884	UGS01414	URS01414	UGO01214	URO01214	yes	yes
Pgm1	Phosphoglucose mutase 1	LD36183	UGS01225	URS01225		URO01332		yes
PHGPx	PHGPx	SD18370	UGS01412	URS01412	UGO01212	URO01212	yes	yes
PhKgamma	Phosphorylase kinase gamma	GH28523	UGS01392	URS01392		URO01092		yes
Pi3K92E	Pi3K92E	SD05105				URO01296		
PIG-A	Phosphatidylinositol glycan anchor biosynthesis class A	LD44262	UGS01211	URS01211		URO01111		yes
Pitslre	Pitslre	LD39519	UGS01436	URS01436	UGO01236	URO01236	yes	yes
Pka-C1	Protein kinase, cAMP-dependent, catalytic subunit 1	LD13640	UGS01342	URS01342	UGO01042	URO01042	yes	yes
Pka-R1	Protein kinase, cAMP-dependent, regulatory subunit type 1	LD43873		URS01210		URO01110		
Pka-R2	Protein kinase, cAMP-dependent, regulatory subunit type 2	LD44591		URS01484		URO01284		
Pkg21D	Protein kinase, cGMP-dependent at 21D	GH03852	UGS01245	URS01245	UGO01329	URO01145	yes	yes
Pnn	Pinin	RE29832		URS01280	UGO01333	URO01180		yes
Pp1-13C	Protein phosphatase 1 at 13C	GH10637	UGS01387	URS01387	UGO01087			yes
Pp1alpha-96A	Protein phosphatase 1alpha at 96A	LD14639	UGS01410	URS01410	UGO01210	URO01210	yes	yes

Pp4-19C	Protein phosphatase 19C	RE58406	UGS01286	URS01286	UGO01186	URO01343	yes	yes
prd	paired	GH22686		URS01320		URO01020		
primo-2	primo-2	AT28881	UGS01296	URS01296	UGO01196	URO01196	yes	yes
Psn	Presenilin	LD23505	UGS01483	URS01483	UGO01283	URO01283	yes	yes
PSR	phosphatidylserine receptor	LD25827	UGS01395	URS01395	UGO01095	URO01095	yes	yes
Ptp61F	Protein tyrosine phosphatase 61F	LP01280	UGS01255	URS01255	UGO01155	URO01155	yes	yes
Pu	Punch	LD37787	UGS01424	URS01424	UGO01224			yes
Rab10	Rab10	LD39986	UGS01446	URS01446	UGO01246	URO01246	yes	yes
Rab11	Rab11	GM06568	UGS01335	URS01335	UGO01307	URO01035	yes	yes
Rab18	Rab18	GH11193	UGS01355	URS01355	UGO01055	URO01055	yes	yes
Rab2	Rab2	GH01619	UGS01361	URS01361		URO01317		yes
Rab21	Rab21	RE42508	UGS01285	URS01285	UGO01185			yes
Rab23	Rab23	RH23273		URS01290				
Rab3	Rab3	LP05860	UGS01454		UGO01254	URO01254		yes
Rab30	Rab30	RE14786	UGS01276	URS01276	UGO01176	URO01176	yes	yes
Rab32	Rab32	LD04613	UGS01330	URS01330	UGO01030	URO01030	yes	yes
Rab35	Rab35	LD21953	UGS01369	URS01369	UGO01069	URO01319	yes	yes
Rab5	Rab5	GH24702	UGS01391	URS01391	UGO01091	URO01091	yes	yes
Rab6	Rab6	GH09086	UGS01384	URS01384		URO01084		yes
Rab7	Rab7	GH03685	UGS01380	URS01380		URO01080		yes
Rab8	Rab8	LD44762	UGS01214	URS01214	UGO01321			yes

Rab9	Rab9	RE17845	UGS01278	URS01278	UGO01178			yes	
Rab9Fb	Rab at 9Fb	IP08727	UGS01427	URS01427	UGO01227	URO01227	yes	yes	
RabX1	RabX1	LD47384	UGS01217	URS01217		URO01117		yes	
RabX6	RabX6	RE70650	UGS01469	URS01469	UGO01269	URO01269	yes	yes	
Rac1	Rac1	LD34217	UGS01438	URS01438		URO01238		yes	★
Rac2	Rac2	GM13874	UGS01346	URS01346	UGO01046	URO01046	yes	yes	
Rack1	Receptor of activated protein kinase C 1	RE74715		URS01288	UGO01188	URO01188		yes	
Raf	Raf oncogene	GH03557	UGS01490	URS01490	UGO01290	URO01290	yes	yes	
Rala	Ras-like protein A	LD21679	UGS01349	URS01349	UGO01049	URO01049	yes	yes	
Ran	Ran	GM14354	UGS01348	URS01348		URO01048		yes	
Rap1	Rap1 GTPase	RE42418	UGS01284	URS01284	UGO01184	URO01184	yes	yes	
Rap2l	Ras-associated protein 2-like	RE63021	UGS01476	URS01476	UGO01276			yes	
ras	raspberry	LD36080	UGS01495		UGO01295	URO01295		yes	
Ras64B	Ras oncogene at 64B	RE36103	UGS01465	URS01465	UGO01265	URO01265	yes	yes	
Rel	Relish	GH01881	UGS01313	URS01313	UGO01013	URO01013	yes	yes	
Rho1	Rho1	GH20776	UGS01364	URS01364	UGO01064	URO01318	yes	yes	
RhoGAP 5A	Rho GTPase activating protein at 5A	SD02309	UGS01218	URS01218	UGO01118	URO01330	yes	yes	★
RhoGDI	RhoGDI	LD16419	UGS01337	URS01337		URO01312		yes	
RnrS	Ribonucleoside diphosphate reductase small subunit	LD41588	UGS01207	URS01207	UGO01107	URO01107	yes	yes	

RpL10	Ribosomal protein L10	RE02339	UGS01433	URS01433		URO01233		yes
RpL13A	Ribosomal protein L13A	GM13948	UGS01347	URS01347	UGO01310	URO01047	yes	yes
RpL40	Ribosomal protein L40	RE10554	UGS01272	URS01272	UGO01172	URO01172	yes	yes
RpS6	Ribosomal protein S6	LD31286	UGS01230	URS01230		URO01334		yes
rush	rush hour	GH19261	UGS01405		UGO01205	URO01205		yes
Sam-S	S-adenosylmethionine Synthetase	LD40460	UGS01428	URS01428	UGO01228	URO01228	yes	yes
scramb1	scramblase 1	GM13876		URS01367		URO01067		
sgg	shaggy	LD44595	UGS01213	URS01213	UGO01113	URO01113	yes	yes
sgl	sugarless	SD09476	UGS01236	URS01236		URO01136		yes
shtd	shattered	LD37115*	UGS01206	URS01206	UGO01319	URO01106	yes	yes
sina	seven in absentia	HL08111	UGS01254		UGO01154	URO01154		yes
Sk1	Sphingosine kinase 1	RE64552	UGS01467		UGO01267	URO01267		yes
Skp2	S-phase kinase-associated protein 2	GM13370 *	UGS01221	URS01221		URO01121		yes
SkpB	SKP1-related B	IP02725	UGS01479	URS01479		URO01279		yes
slmb	supernumerary limbs	LD08669	UGS01240	URS01240	UGO01140	URO01140	yes	yes
Smox	Smad on X	LD15813			UGO01018	URO01308		yes
sn	singed	RH62992	UGS01470	URS01470	UGO01270	URO01270	yes	yes
Sod2	Superoxide dismutase 2 (Mn)	GH02759	UGS01352	URS01352	UGO01052	URO01052	yes	yes
Spps	Sp1-like factor for pairing sensitive-silencing	LD04007	UGS01323	URS01323		URO01023		yes
Sptr	Sepiapterin reductase	GH04031	UGS01353		UGO01053	URO01053		yes

sqa	spaghetti-squash activator	GH17420	UGS01449	URS01449	UGO01249	URO01249	yes	yes
sqh	spaghetti squash	LD14743	UGS01231	URS01231	UGO01131	URO01335	yes	yes
Src64B	Src oncogene at 64B	LD30429			UGO01291			
SREBP	Sterol regulatory element binding protein	LP12374	UGS01314		UGO01014	URO01014		yes
STUB1	STIP1 homology and U-box containing protein 1	RE01069	UGS01268	URS01268	UGO01168	URO01168	yes	yes
Su(var)2-10	Suppressor of variegation 2-10	RE73180	UGS01474	URS01474	UGO01274			yes
Su(var)2-10	Suppressor of variegation 2-10	RE55465	UGS01437	URS01437	UGO01237	URO01237	yes	yes
Su(var)3-3	Suppressor of variegation 3-3	LD45081	UGS01264	URS01264	UGO01164			yes
Su(z)12	Su(z)12	SD04959			UGO01166	URO01166		yes
Swip-1	Swiprosin-1	SD04693	UGS01226	URS01226	UGO01126	URO01333	yes	yes
Syb	Synaptobrevin	SD05285	UGS01425	URS01425	UGO01225	URO01225	yes	yes
Synd	Syndapin	LD46328		URS01216	UGO01323	URO01116		yes
Syx1A	Syntaxin 1A	LD43943	UGS01222	URS01222	UGO01122	URO01122	yes	yes
Tace	Tace	RE65757	UGS01413	URS01413	UGO01213	URO01213	yes	yes
Tak1	TGF-β activated kinase 1	LD42274	UGS01253	URS01253	UGO01153	URO01153	yes	yes
Tango4	Transport and Golgi organization 4	LD24662		URS01374		URO01322		
Taz	Tafazzin	RE14108	UGS01274	URS01274		URO01341		yes
TBCB	tubulin-binding cofactor B	LD45244	UGS01359	URS01359	UGO01059	URO01059	yes	yes

Tbp	TATA binding protein	LD44083	UGS01304	URS01304	UGO01004	URO01004	yes	yes
Tcs3	Tcs3	RE13621	UGS01273	URS01273	UGO01173	URO01340	yes	yes
TfAP-2	Transcription factor AP-2	RE17884	UGS01308	URS01308	UGO01008			yes
Tfb1	Transcription factor B1	SD04652			UGO01024	URO01024		yes
Tg	Transglutaminase	RE08173		URS01432	UGO01232	URO01232		yes
Tip60	Tat interactive protein 60kDa	LD31064	UGS01249	URS01249	UGO01149	URO01149	yes	yes
tmod	tropomodulin	GH23271	UGS01390	URS01390	UGO01090	URO01090	yes	yes
Traf4	TNF-receptor-associated factor 4	LD20987	UGS01338	URS01338	UGO01038	URO01038	yes	yes
Traf6	TNF-receptor-associated factor 6	GH01161	UGS01376		UGO01076	URO01076		yes
Tsc1	Tsc1	LD23779		URS01451	UGO01251	URO01251		yes
Tsp66E	Tetraspanin 66E	RE39068	UGS01283	URS01283	UGO01183	URO01183	yes	yes
Tsp96F	Tetraspanin 96F	LD19727	UGS01327	URS01327		URO01027		yes
Ubc10	Ubiquitin conjugating enzyme 10	RE47264	UGS01475	URS01475	UGO01275	URO01275	yes	yes
Ube3a	Ubiquitin protein ligase E3A	LD21888	UGS01459	URS01459	UGO01259	URO01259	yes	yes
Ufd1-like	Ubiquitin fusion-degradation 1-like	GH18603	UGS01356	URS01356	UGO01056	URO01316	yes	yes
Uros1	Uroporphyrinogen III synthase 1	GH17465	UGS01363	URS01363		URO01063		yes
usp	ultraspiracle	LD09973	UGS01343	URS01343	UGO01043			yes
Vav	Vav guanine nucleotide exchange factor	LD25754	UGS01456	URS01456	UGO01256			yes
Vinc	Vinculin	SD03117	UGS01457	URS01457	UGO01257	URO01257	yes	yes
Vps28	Vacuolar protein sorting 28	GH04443	UGS01381	URS01381	UGO01081			yes

WASp	WASp	RE12101	UGS01461	URS01461	UGO01261	URO01261	yes	yes	★
wbl	windbeutel	IP02648	UGS01480		UGO01280	URO01280		yes	
Wdfy2	WD repeat and FYVE domain containing 2	LD41958	UGS01208	URS01208	UGO01320	URO01108	yes	yes	
Wwox	WW domain containing oxidoreductase	LD03827	UGS01329		UGO01305			yes	
zda	zonda	LD36412		URS01205	UGO01105	URO01105		yes	

Table 3. Production steps. [**]

Production steps	Attempted	Obtained	Success	Note
(*1*) Construct production.	286 proteins with 4-way labeling equals a total of 1144 expression constructs.	988 expression constructs.	83% for 4-way. 97% for 2-way.	2-way labeling is most likely sufficient for checking possible interactions *in vivo*.
(*2*) Genome transformation.	32 proteins (128 4-way labeled transgenes) selected from (*1*).	All 128 homozygous single transgenic stock lines.	100%.	Transformation of transgenes into the *Drosophila* genome is straightforward.
(*3*) Stock construction.	Only 11 protein-protein links in (*2*) had their binding compatibility demonstrated biochemically; besides the Cdc42-to-WASp link (see Sharifai et al., 2014), the remaining 10 links were yet to be characterized *in vivo*.	18 double homozygous and 4 triple homozygous stock lines (see **Table 4**).	100%.	Establishing GAL4-responsive double and triple transgenic stock lines is straightforward.
(*4*) Sample visualization.	Triple transgenic stocks from (*3*) were crossed to a pan-neuronal *elav-GAL4* driver. Eggs were then collected and raised subsequently through larval stages.	Embryos developed normally without any apparent anomaly in anatomy or behavior until third instar larval stage.	76%.	Nearly the same viability as in the previous report on double transgene stocks (Sharifai et al. 2014).

[**] In terms of production difficulty, transgene creation step (*1*) is the toughest and subsequent steps (*2*) through (*4*) are all forthright. In terms of time and cost of ultimately charting the map, however, step (*4*) can be the most extensive. Pre-selection of protein-protein links that are likely to produce FRET in the native environment is recommended.

Table 4. *Drosophila* stocks. ††

Stock	Co-expression	Genotype	FRET
1	Cdc42 *blank*	UAS-WASp::eGFP UAS- mCherry	
2	Cdc42 WASp	UAS-eGFP::Cdc42 UAS-mCherry::WASp	★
3	Cdc42 WASp	UAS-eGFP::Cdc42 UAS-WASp::mCherry	★
4	Cdc42 WASp	UAS-Cdc42::eGFP UAS-mCherry::WASp	★
5	Cdc42 WASp	UAS-Cdc42::eGFP UAS-WASp::mCherry	★
6	WASp Cdc42	UAS-eGFP::WASp UAS-mCherry::Cdc42	★
7	WASp Cdc42	UAS-eGFP::WASp UAS-Cdc42::mCherry	★
8	WASp Cdc42	UAS-WASp::eGFP UAS-Cdc42::mCherry	★

†† Double and triple homozygous stocks of GAL4-responsive transgenes are ready for characterizing possible interactions between Cdc42 and its effectors WASp (2-8,19), Par6 (12,14,15,19,21) or Pak1 (19). Here, multiple tag positions and FRET directionalities may be assessed for interaction between Cdc42 and WASp, and similarly for interaction between Cdc42 and Par6. In each case, the magenta box indicates whether the FRET donor, either eGFP or mCherry, possibly undergoes a decrease in fluorescence lifetime if in near field proximity to the FRET acceptor-labeled POI. An important 'negative' control yielding no FRET is to co-express eGFP-labeled Cdc42 along with unfused mCherry (1), which is especially important for assessing positive FRET with mCherry-labeled WASp, Par6 or RhoGAP (13). In addition to Cdc42, possible interactions between Rac1, another Rho subfamily monomeric G protein, and WASp (17,21), Par6 (16,22) or Pak1 (18) are also ready for experimentation. WASp, incidentally, has potential interaction with Arp3 (9-11). With the trio of labels, the potential of completive interactions between a single G protein for two mutually exclusive partners Pak1 and WASp (19), or similarly between Pak1 and Par6 (20), may be revealed within the same animals. Alternatively, the same can be done for two G proteins Cdc42 and Rac1 competing for a common effector such as WASp (21) or Par6 (22). *Asterisks* (★ and ★) indicate possible detection of FRET between one or two pairs of proteins. (*Note:* To request any of these 22 double or triple transgenic homozygous stocks from Chiba lab, genotypes are required.) **[genetics_table]**

9		UAS-WASp::eGFP UAS-mCherry::Arp3	★
10	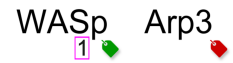	UAS-WASp::eGFP UAS-Arp3::mCherry	★
11		UAS-Arp3::eGFP UAS-mCherry::WASp	★
12	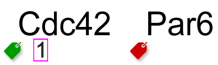	UAS-eGFP::Cdc42 UAS-mCherry::Par6	★
13		UAS-eGFP::Cdc42 UAS-mCherry::RhoGAP	★
14		UAS-eGFP::Par6 UAS-mCherry::Cdc42	★
15		UAS-mCherry::Par6 ; UAS-Cdc42::NirFP	★
16		UAS-eGFP::Par6 UAS-mCherry::Rac1	★
17	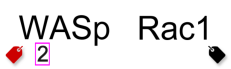	UAS-mCherry::WASp ; UAS-Rac1::NirFP	★
18	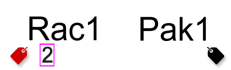	UAS-mCherry::Rac1 ; UAS-Pak1::NirFP	★
19		UAS-eGFP::WASp UAS-mCherry::Cdc42 ; UAS-NirFP::Pak1	★★
20	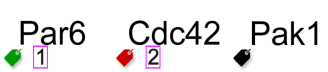	UAS-eGFP::Par6 UAS-mCherry::Cdc42 ; UAS-NirFP::Pak1	★★
21		UAS-eGFP::Cdc42 UAS-mCherry::WASp ; UAS-Rac1::NirFP	★★
22		UAS-eGFP::Cdc42 UAS-mCherry::Par6 ; UAS-Rac1::NirFP	★★

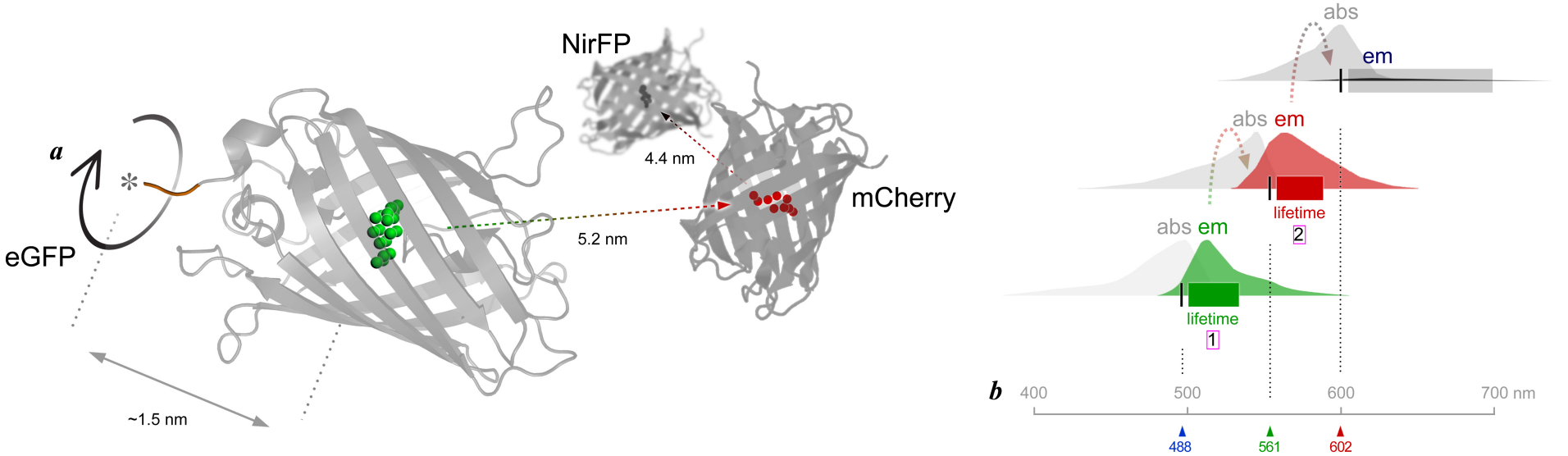

Figure 1. Labels. (***a***) Structures of fluorescent labels. Monomeric eGFP has twenty-two atoms (green) fluoresce together at the center of a "cage" — a rigid barrel structure composed of eleven anti-parallel ß sheets.The distance from the center of this α helical fluorophore to the edge of a protein of interest (gray *asterisk*) is about 1.5 nm. eGFP's carboxyl terminus with an additional 17-mer polypeptide (brown) exhibits a great deal of flexibility, (circle *arc*). This "loop" is anticipated to randomize the polar orientation κ^2 of eGFP in respect to the protein it labels, thereby dramatically simplifying the computation of Förster resonance energy transfer that may occur between different fluorescent labels. The emission of eGFP and the absorption of mCherry display extensive spectral overlap (see *(b)*), providing a possibility of FRET with the Förster distance of 5.2 nm between these two fluorophores. Monomeric mCherry also has fluorescing ions (red) surrounded by a barrel composed of anti-parallel ß sheets. Its emission and the absorption of NirFP display generous spectral overlap (see *(b)*) and provide a possibility of FRET with a Förster distance of 4.4 nm between these two fluorophores. The detailed structure of NirFP remains currently unknown. (***b***) Spectra of fluorescent labels. With a 488 nm diode laser (blue *arrowhead*), eGFP fluorescence (green *bar*) may be examined with its lifetime τ of 2.56 ns. Its emission (green *spectrum*) and the absorption of mCherry (gray *spectrum*) overlap. If any physical interaction between proteins *A* and *B* occurs, this induces FRET between the two fluorophores. Hence, shortening of the lifetime τ of the FRET donor eGFP (magenta *box1*) signifies FRET. With a 561 nm diode laser (green *arrowhead*), mCherry fluorescence (red *bar*) may be examined with its normal lifetime τ of 1.47 ns. Its emission (red *spectrum*) and the absorption of NirFP (gray *spectrum*) overlap. If any physical interaction occurs between proteins *B* and *C,* this induces FRET between the two fluorophores. With a 602 nm diode laser (red *arrowhead*), NirFP fluorescence (gray *bar*) may be examined. The crystal structure of NirFP is currently unavailable. **<339> green: 009900, red: cc3300, black: 000000** **[labels_new / 12>>10]**

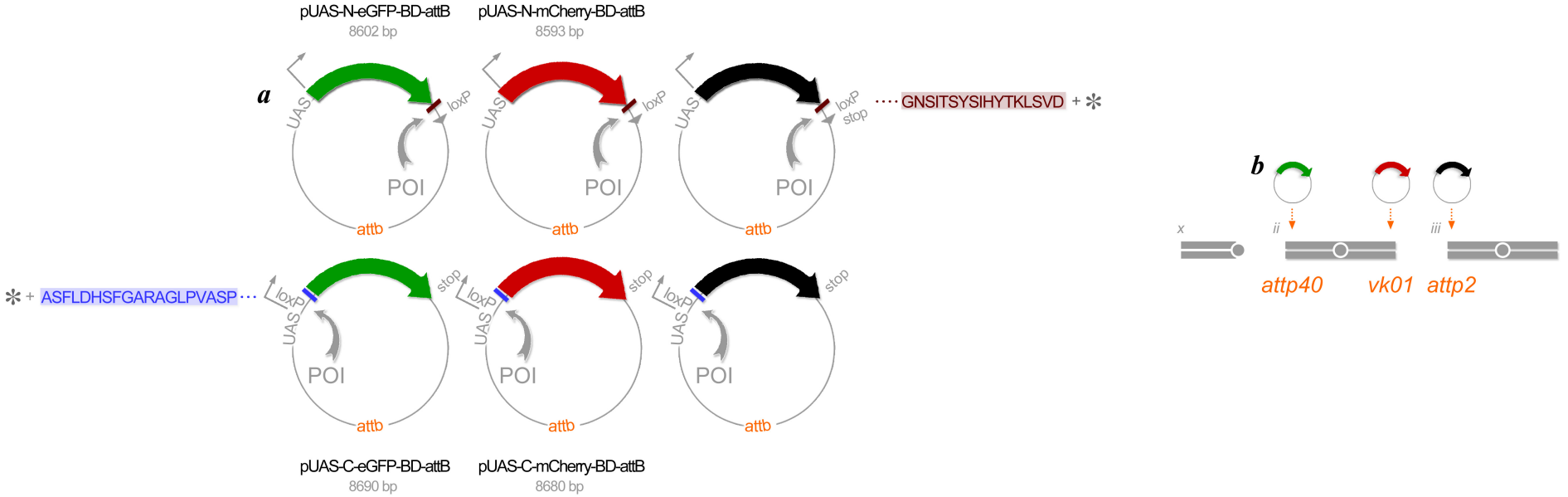

Figure 2. Transformation. (***a***) Expression vectors. Constructed in *E. coli* plasmids in six complementary manners, an individual protein of interest (POI) (gray *arc*) is labeled at either its amino terminus (top row) or its carboxyl terminus (bottom row) with eGFP (green), mCherry (red) or NirFP (black). A short, flexible polypeptide sequence (brown or purple *bar*) between the protein (gray *asterisk*) and its fluorescent label is added to randomize the dipole orientations when a pair of labeled proteins are being assessed for possible interaction via FRET occurrence. All these expression vectors are placed downstream of the *UAS* sequence for expressing the labeled proteins under the GAL4 expression system, and also carry the *attb* sequence for PhiC31-mediated genomic integration to specific landing sites (see *(b)*). All plasmids carry mini w^+ as a transformation marker (not shown). (***b***) Genomic integration. PhiC31 integrase enables position-specific genomic integration of all transgenes for eGFP-labeled proteins to the landing site *attp40* on the second chromosome, all transgenes for mCherry-labeled proteins to the landing site *vk01* on the chromosome 2, and all transgenes for NirFP-labeled proteins to landing site *attp2* on the chromosome 3. <186> **brown: 660000, purple: 3333ff, blue 0066ff, orange ff6600** [transformation_new/ 12>>10]

Single

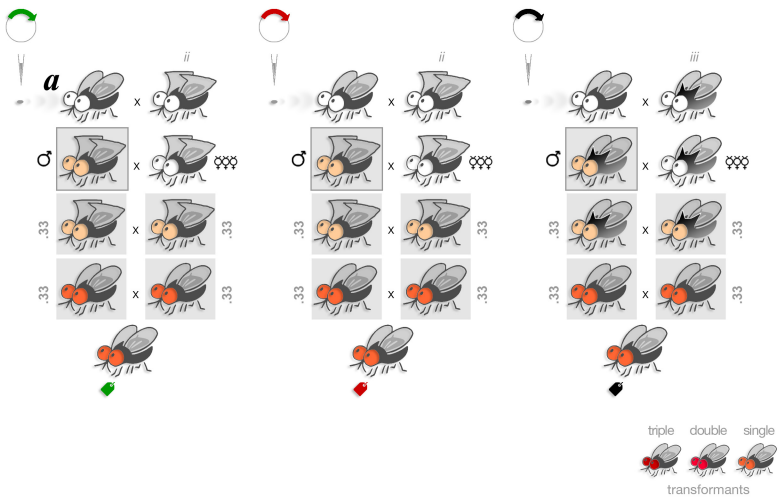

Double

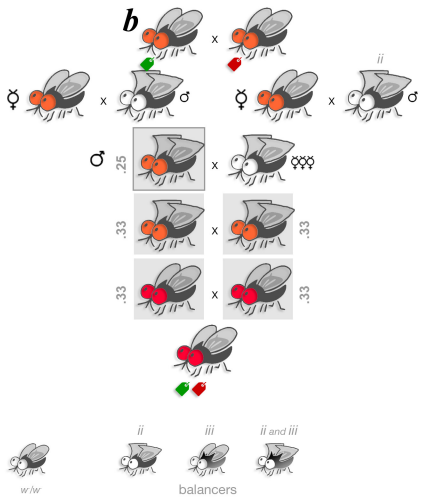

Triple

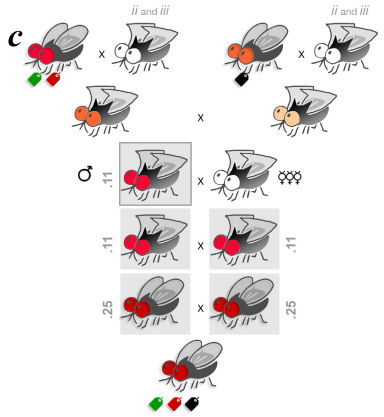

Co-localization

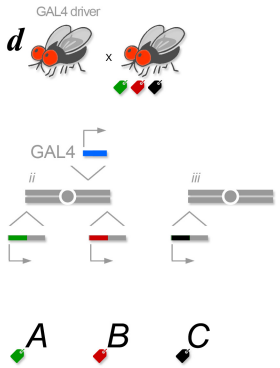

Interaction

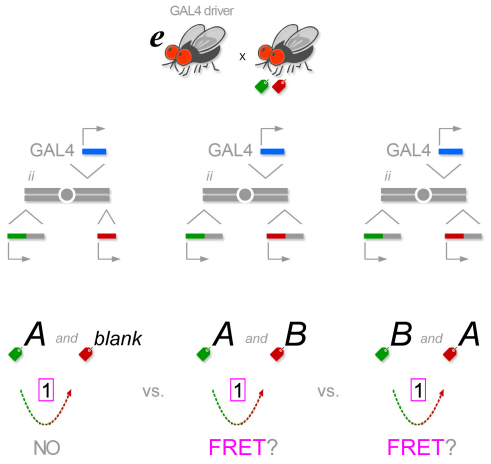

Figure 3. *Drosophila* genetics. (***a***) Single transgene stocks express proteins that are eGFP-labeled (*left*), mCherry-labeled (*center*) or NirFP-labeled (*right*). Five generations will: (1) integrate fluorescently labeled protein of interest (see **FIG2***a*), (2) recover transformant as a single heterozygous male, (3) expand, (4) homozygose, then (5) stock. The PhiC31-mediated genomic integration into *Drosophila* genome (see **FIG2***b*) occurs at a rate of approximately 2% in each sex. Generations (2) through (4) establish stock genotype with 100% confidence. When a given cross results in mixed genotypes, only those with certain genotypes are used (gray *boxes*). Probability expected using Mendelian genetics (gray *number*) and externally visible markers such as the color of eye and the shape of wing and/or hair on back cuticle are indicated. (***b***) Double transgene stocks co-express pairs of proteins that are eGFP-labeled and mCherry-labeled. Six generations will: (1) combine two transgenes on chromosome *ii* through homologous recombination, (2) cross several single females in parallel, (3) recover transformant as a single heterozygous male, (4) expand, (5) homozygose, then (6) stock. Homologous recombinations occur in the germ line of females, but balancer chromosomes suppress any such occurrence. If a virgin female mates with a male carrying the balancer for chromosome *ii*, the chance of having two transgenes on this chromosome homologously recombine with each other will be virtually 50:50. The expected offspring ratio in generation (3) will be either 50% red and 50% white in eye color with or without the balancer, or alternatively all barely red regardless of their wing being curly or not. (***c***) Triple transgene stocks co-express trios of proteins that are eGFP-labeled, mCherry-labeled and NirFP-labeled. Six generations will: (1) re-balance a double transgene stock on chromosome *ii* (*left*) and a single transgene stock on chromosome *iii* (*right*), (2) combine the three transgenes while suppressing any homologous recombination on either chromosome, (3) recover transformant as a single male, (4) expand, (5) homozygose, then (6) stock. Similar six generations of crosses starting with a single transgene stock of mCherry-labeled protein and a single transgene stock of NirFP-labeled protein establish a double transgene stock (not shown). All animals are of w^{-}/w^{-} background and, therefore, their eye colors reflect the number of transgenes they carry. Balancer for chromosome 2 (*ii*) carries $Cy^{'}$ mutation that causes wings to curl, and chromosome 3 (*iii*) carries $Sb^{'}$ mutation that causes hair on back cuticle to thicken. (***d***) Co-localization of proteins *A, B* and *C*. Three proteins labeled with eGFP, mCherry and NirFP, respectively, under the control of a GAL4 driver in embryos/larvae may be imaged by crossing fathers carrying the GAL4 driver to mothers from a triple transgene stock (see *(c)*). (***e***) Possible interaction between proteins *A* and *B*. Embryos/larvae may be imaged by crossing fathers carrying the GAL4 driver to mothers from a double transgene stock for labeling proteins with eGFP and mCherry (see *(b)*). FRET between eGFP and mCherry are considered evidence for physical interaction between the proteins *A* and *B*. Such an interaction possibility can be further confirmed through reciprocal labeling for this protein pair. Negative control (*no FRET*) to be run in parallel is eGFP-labeled protein *A* expressed along with "*blank*" cytoplasmic mCherry. **<522> half:ffcc99, full:ff6633, more ff0033, even more:cc0000** **[new_genetics / 12>>10]**

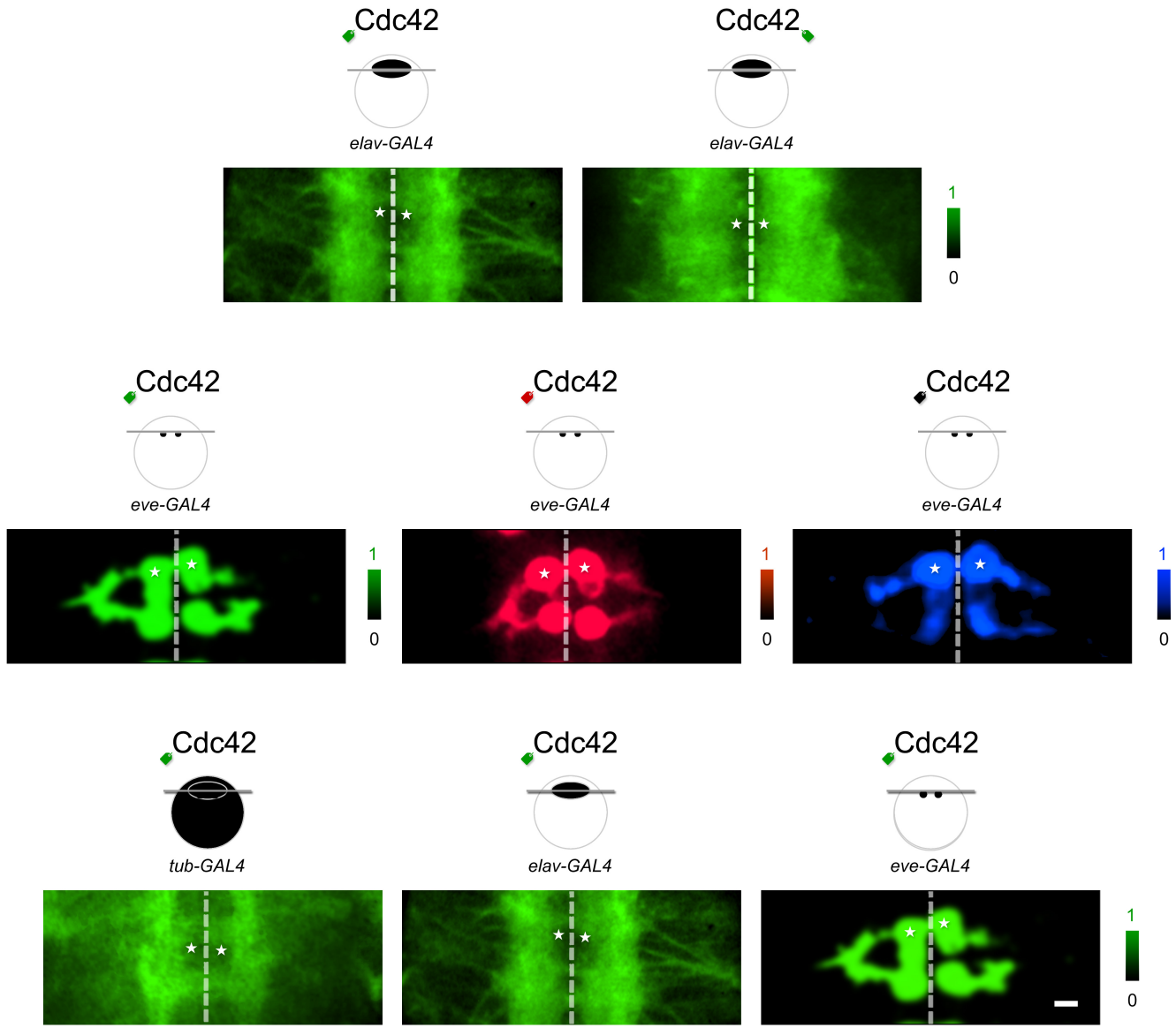
Cdc42
elav-GAL4
Cdc42
elav-GAL4
1
0
Cdc42
eve-GAL4
Cdc42
eve-GAL4
Cdc42
eve-GAL4
1
0
1
0
1
0
Cdc42
tub-GAL4
Cdc42
elav-GAL4
Cdc42
eve-GAL4
1
0

Figure 4. Expression control. (***a***) Label may be fused to either amino or carboxyl terminus of protein of interest. In our experience, both the amino or carboxyl termini labeling were indistinguishable. Genotypes: *UAS-eGFP::Cdc42 / elav-GAL4* (*left*), *UAS-Cdc42::eGFP / elav-GAL4* (*right*). (***b***) Label may adopt either a green color with eGFP (*left*), a red color with mCherry (*middle*) or a black (purple) with NirFP (*right*). Genotypes: *UAS-eGFP::Cdc42 / eve-GAL4* (*left*), *UAS-mCherry::Cdc42 / eve-GAL4* (*middle*), + / *eve-GAL4 ; UAS-NirFP::Cdc42 /* + (*right*). Again, colors do not seem to impact the way proteins distribute within the animals. (***c***) Labeled proteins may be expressed either ubiquitously using *tub-GAL4* (*left*), pan-neuronally using *elav-GAL4* (*middle*) or cell specifically using *eve-GAL4* (*right*). Genotypes: *UAS-eGFP::Cdc42 / tub-GAL4* (*left*), *UAS-eGFP::Cdc42 / elav-GAL4* (*middle*), *UAS-eGFP::Cdc42 / eve-GAL4* (*right*). Dashed lines indicate the midline. Asterisks point to the cell bodies of the bilateral pair of aCC motoneurons in the abdominal segment 3. Scale bar 10 nm. **<156>** **<previous page>** **[control / 12>>10]**

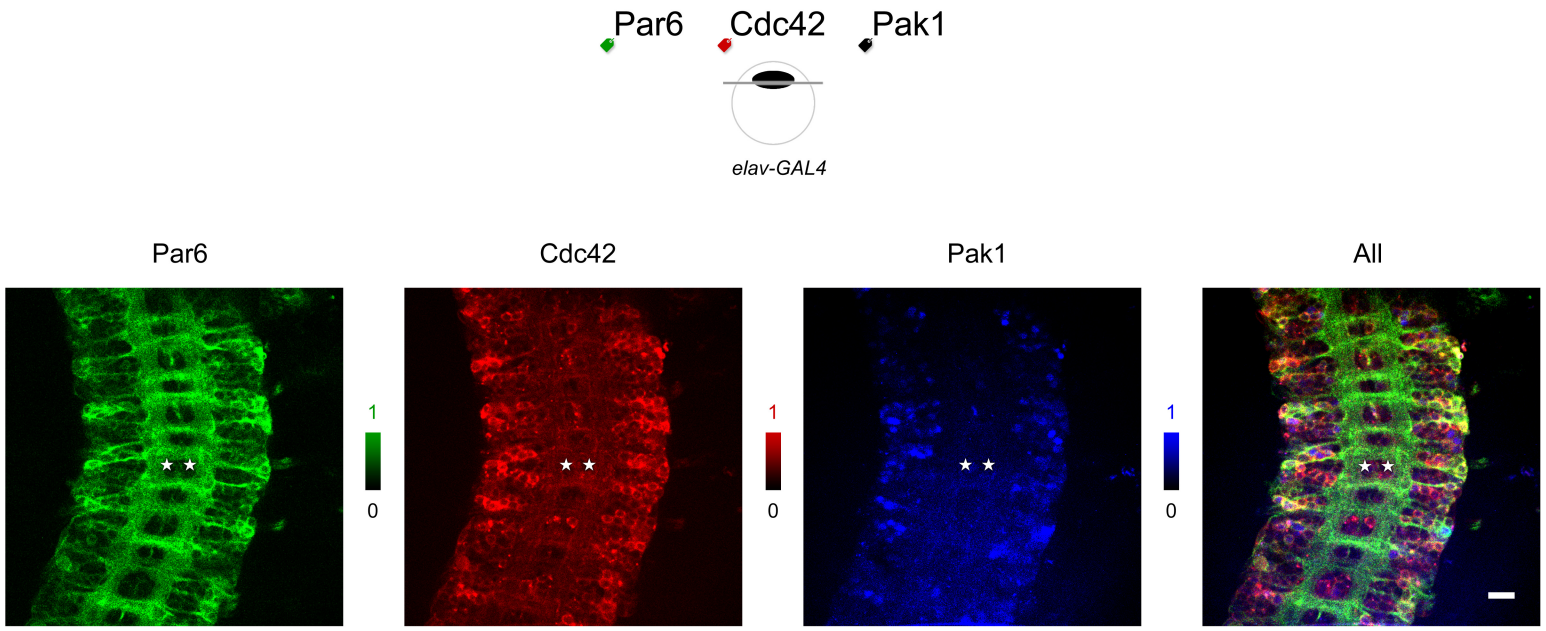

Figure 5. Co-localization of *A, B* and C. eGFP-labeled Par6 (green), mCherry-labeled Cdc42 (red), and NirFP-labeled Pak1 (blue *pixels*) are co-expressed in all neurons of a *Drosophila* embryo. Their expression patterns vary from pixel to pixel and from cell to cell. Anatomical features help identify a bilateral pair of aCC motoneurons (*asterisks*) in the abdominal segment A2. Genotype: *UAS-eGFP::Par6 UAS-mCherry::Cdc42 / elav-GAL4 ; UAS-NirFP::Pak1 / +*. Scale bar 20 nm. **<70>** **[trio_new / 12>>10]** **black/purple: 0033ff**

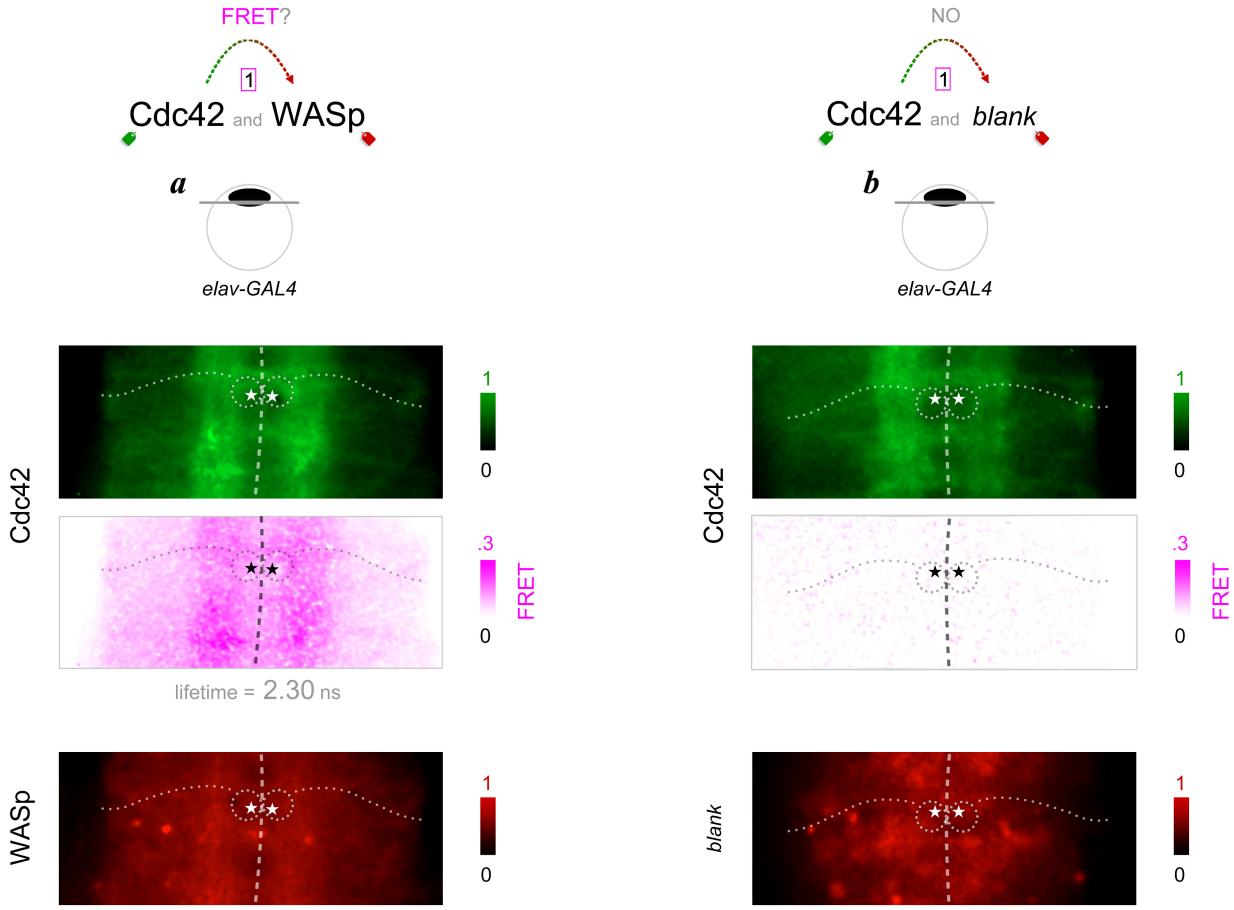

Figure 6. Interaction between *A* and *B*. (***a***) Interaction between monomeric G protein Cdc42 and its alleged partner WASp is revealed by FRET. Cdc42 is present at higher concentrations in neuropil region near the midline (dashed line) compared to cortical region (*top* panel). Probability of FRET between eGFP and mCherry that labels Cdc42 and WASp, respectively, is higher in the neuropil (*middle* panel). Estimated FRET probability of .24 here translates to about one in four eGFP-labeled Cdc42 proteins are within the FRET-able proximity to mCherry-labeled WASp proteins. *Asterisks* show where the bilateral pair of aCC motoneuron cell bodies are located. Their axons (dotted lines) extend laterally through first the neuropil region with higher FRET and then out into the cortical region with lower FRET. Distribution pattern of WASp, meanwhile, is distinct from Cdc42's (*bottom* panel). However, the expression patterns of Cdc42 and WASp as well as their co-expression do not correlate to the observed FRET pattern. (***b***) Control intended for no FRET detection. The mean eGFP fluorescence lifetime at the neuropil stays at 2.56 ns, indicating no FRET. Genotype: *UAS-eGFP::Cdc42 UAS-WASp::mCherry / elav-GAL4* in (*a*) and *UAS-eGFP::Cdc42 UAS-mCherry / elav-GAL4* in (*b*). **<192>** **[intereaction_new / 12>>10]**

Gene Symbol	Gene Name	Transcript-ID	CG	FBgn_ID
Act42A	Actin 42A	Act42A-RA	CG12051	FBgn0000043
Act5C	Actin 5C	Act5C-RA	CG4027	FBgn0000042
Actn	alpha actinin	Actn-RA	CG4376	FBgn0000667
AdenoK	Adenosine Kinase	AdenoK-RA	CG11255	FBgn0036337
ago	archipelago	ago-RA	CG15010	FBgn0041171
Agpat1	;lycerol-3-phosphate O-acyltransf	Agpat1-RA	CG3812	FBgn0030421
ALiX	ALG-2 interacting protein X	ALiX-RA	CG12876	FBgn0086346
alph	alphabet	alph-RE	CG1906	FBgn0086361
amon	amontillado	amon-RA	CG6438	FBgn0023179
AnxB9	Annexin B9	AnxB9-RB	CG5730	FBgn0000083
APC10	phase Promoting Complex subuni	APC10-RA	CG11419	FBgn0034231
Aplip1	?P-like protein interacting protein	Aplip1-RB	CG1200	FBgn0040281
Aplip1	?P-like protein interacting protein	Aplip1-RA	CG1200	FBgn0040281
Appl	eta amyloid protein precursor-lik	Appl-RA	CG7727	FBgn0000108
Arf51F	ADP ribosylation factor at 51F	Arf51F-RA	CG8156	FBgn0013750
Arf79F	ADP ribosylation factor at 79F	Arf79F-RA	CG8385	FBgn0010348
ArfGAP3	sylation factor GTPase activating	ArfGAP3-RA	CG6838	FBgn0037182
Arp2	Actin-related protein 2	Arp2-RA	CG9901	FBgn0011742
Arp3	Actin-related protein 3	Arp3-RA	CG7558	FBgn0262716
Arpc2	·related protein 2/3 complex, sub	Arpc2-RA	CG10954	FBgn0032859
Arpc3B	elated protein 2/3 complex, subu	Arpc3B-RA	CG8936	FBgn0065032
Arpc5	·related protein 2/3 complex, sub	Arpc5-RA	CG9881	FBgn0031437
Ate1	Arginyltransferase 1	Ate1-RA	CG9204	FBgn0025720
Ate1	Arginyltransferase 1	Ate1-RB	CG9204	FBgn0025720
Atg8a	Autophagy-related 8a	Atg8a-RA	CG32672	FBgn0052672
ATPsynB	ATP synthase, subunit B	ATPsynB-RA	CG8189	FBgn0019644
ATPsynbeta	ATP synthase, beta subunit	ATPsynbeta-RA	CG11154	FBgn0010217
ATPsyndelta	ATP synthase, delta subunit	ATPsyndelta-RA	CG2968	FBgn0028342
ATPsynG	ATP synthase, subunit G	ATPsynG-RA	CG6105	FBgn0010612
ATPsyngamma	ATP synthase, gamma subunit	ATPsyngamma-RA	CG7610	FBgn0020235
ATPsynO	ıse, oligomycin sensitivity conferr	ATPsynO-RA	CG4307	FBgn0016691
ball	ballchen	ball-RA	CG6386	FBgn0027889
betaTub56D	beta-Tubulin at 56D	betaTub56D-RB	CG9277	FBgn0284243
betaTub85D	beta-Tubulin at 85D	betaTub85D-RA	CG9359	FBgn0003889
blw	bellwether	blw-RA	CG3612	FBgn0011211
boi	brother of ihog	boi-RA	CG32796	FBgn0040388
bru1	bruno 1	bru1-RA	CG31762	FBgn0000114
bs	blistered	bs-RA	CG3411	FBgn0004101

bsk	basket	bsk-RB	CG5680	FBgn0000229
Btk29A	Btk family kinase at 29A	Btk29A-RB	CG8049	FBgn0003502
Buffy	Buffy	Buffy-RA	CG8238	FBgn0040491
cact	cactus	cact-RA	CG5848	FBgn0000250
CanA1	Calcineurin A1	CanA1-RA	CG1455	FBgn0010015
CCT6	aperonin containing TCP1 subuni	CCT6-RA	CG8231	FBgn0027329
Cdc23	Cell division cycle 23	Cdc23-RA	CG2508	FBgn0032863
Cdc27	Cell division cycle 27	Cdc27-RA	CG8610	FBgn0012058
Cdc42	Cell division cycle 42	Cdc42-RA	CG12530	FBgn0010341
CDC45L	CDC45L	CDC45L-RA	CG3658	FBgn0026143
Cdk1	Cyclin-dependent kinase 1	Cdk1-RA	CG5363	FBgn0004106
CG10077	-	CG10077-RA	CG10077	FBgn0035720
CG10298	-	CG10298-RA	CG10298	FBgn0037432
CG11583	-	CG11583-RA	CG11583	FBgn0035524
CG11807	-	CG11807-RA	CG11807	FBgn0033996
CG13887	-	CG13887-RB	CG13887	FBgn0035165
CG17739	-	CG17739-RA	CG17739	FBgn0033710
CG1909	-	CG1909-RA	CG1909	FBgn0039911
CG2862	-	CG2862-RA	CG2862	FBgn0031459
CG3008	-	CG3008-RA	CG3008	FBgn0031643
CG31457	-	CG31457-RB	CG31457	FBgn0051457
CG32137	-	CG32137-RB	CG32137	FBgn0052137
CG3529	-	CG3529-RB	CG3529	FBgn0035995
CG3788	-	CG3788-RA	CG3788	FBgn0034800
CG42540	-	CG42540-RB	CG42540	FBgn0260657
CG7220	-	CG7220-RA	CG7220	FBgn0033544
CG8199	-	CG8199-RA	CG8199	FBgn0037709
CG9281	-	CG9281-RB	CG9281	FBgn0030672
Chc	Clathrin heavy chain	Chc-RC	CG9012	FBgn0000319
cin	cinnamon	cin-RA	CG2945	FBgn0000316
Cka	Connector of kinase to AP-1	Cka-RA	CG7392	FBgn0044323
CkIIbeta	Casein kinase II beta subunit	CkIIbeta-RB	CG15224	FBgn0000259
Cortactin	Cortactin	Cortactin-RA	CG3637	FBgn0025865
COX4L	ytochrome c oxidase subunit 4-lik	COX4L-RA	CG10396	FBgn0033020
Crk	Crk oncogene	Crk-RA	CG1587	FBgn0024811
csul	capsuleen	csul-RA	CG3730	FBgn0015925
csw	corkscrew	csw-RA	CG3954	FBgn0000382
CtsB1	Cathepsin B1	CtsB1-RA	CG10992	FBgn0030521
CycA	Cyclin A	CycA-RA	CG5940	FBgn0000404
CycC	Cyclin C	CycC-RA	CG7281	FBgn0004597
CycD	Cyclin D	CycD-RD	CG9096	FBgn0010315

CycG	Cyclin G	CycG-RA	CG11525	FBgn0039858
Diap2	th-associated inhibitor of apopto	Diap2-RA	CG8293	FBgn0015247
dj-1β	#N/A	dj-1β-RA	CG1349	FBgn0039802
dnr1	defense repressor 1	dnr1-RA	CG12489	FBgn0260866
dock	dreadlocks	dock-RB	CG3727	FBgn0010583
drk	downstream of receptor kinase	drk-RA	CG6033	FBgn0004638
Dsor1	Downstream of raf1	Dsor1-RA	CG15793	FBgn0010269
Dsp1	Dorsal switch protein 1	Dsp1-RA	CG12223	FBgn0278608
E(z)	Enhancer of zeste	E(z)-RA	CG6502	FBgn0000629
Eaat2	xcitatory amino acid transporter	Eaat2	CG3159	FBgn0026438
eIF4B	aryotic translation initiation facto	eIF4B-RA	CG10837	FBgn0020660
eIF4E1	ıryotic translation initiation factor	eIF4E1-RC	CG4035	FBgn0015218
Ent1	uilibrative nucleoside transporte	Ent1-RA	CG11907	FBgn0031250
exd	extradenticle	exd-RA	CG8933	FBgn0000611
FeCH	Ferrochelatase	FeCH-RC	CG2098	FBgn0266268
FeCH	Ferrochelatase	FeCH-RB	CG2098	FBgn0266268
Flo1	Flotillin 1	Flo1-RA	CG8200	FBgn0024754
Flo2	Flotillin 2	Flo2-RM	CG32593	FBgn0264078
Flo2	Flotillin 2	Flo2-RB	CG32593	FBgn0264078
flw	flapwing	flw-RA	CG2096	FBgn0000711
Fnta	Farnesyl transferase alpha	Fnta-RA	CG2976	FBgn0031633
fzr	fizzy-related	rap-RA	CG3000	FBgn0262699
Gad1	Glutamic acid decarboxylase 1	Gad1-RA	CG14994	FBgn0004516
Galphai	G protein alpha i subunit	Galphai-RA	CG10060	FBgn0001104
Galphao	G protein alpha o subunit	Galphao-RA	CG2204	FBgn0001122
Galphas	G protein alpha s subunit	Galphas-RB	CG2835	FBgn0001123
gammaCOP	Coat Protein (coatomer) gamma	gammaCOP-RB	CG1528	FBgn0028968
Gbeta13F	G protein beta-subunit 13F	Gbeta13F-RA	CG10545	FBgn0001105
Gbeta5	Gbeta5	Gbeta5-RA	CG10763	FBgn0030011
Gdi	GDP dissociation inhibitor	Gdi-RA	CG4422	FBgn0004868
GMF	Glia maturation factor	GMF-RA	CG5869	FBgn0028894
Gp93	Glycoprotein 93	Gp93-RA	CG5520	FBgn0039562
grn	grain	grn-RA	CG9656	FBgn0001138
gsb-n	gooseberry-neuro	gsb-n-RA	CG2692	FBgn0001147
gus	gustavus	gus-RA	CG2944	FBgn0026238
Gyg	Glycogenin	Gyg-RB	CG44244	FBgn0265191
h	hairy	h-RA	CG6494	FBgn0001168
HDAC1	Histone deacetylase 1	HDAC1-RA	CG7471	FBgn0015805
HDAC3	Histone deacetylase 3	Hdac3-RA	CG2128	FBgn0025825
HDAC6	Histone deacetylase 6	HDAC6-RA	CG6170	FBgn0026428
Hex-C	Hexokinase C	Hex-C-RA	CG8094	FBgn0001187

Hmgs	HMG Coenzyme A synthase	Hmgs-RA	CG4311	FBgn0010611
Hnf4	Hepatocyte nuclear factor 4	Hnf4-RA	CG9310	FBgn0004914
Hpd	ıydroxyphenylpyruvate dioxygena	Hpd-RB	CG11796	FBgn0036992
Hpd	ıydroxyphenylpyruvate dioxygena	Hpd-RA	CG11796	FBgn0036992
Hr96	Hormone receptor-like in 96	Hr96-RA	CG11783	FBgn0015240
Hrb87F	;eneous nuclear ribonucleoprotei	Hrb87F-RA	CG12749	FBgn0004237
HtrA2	HTRA2-related serine protease	HtrA2-RA	CG8464	FBgn0038233
I-2	Inhibitor-2	I-2-RA	CG10574	FBgn0028429
ICA69	Islet cell autoantigen 69 kDa	ICA69-RA	CG10566	FBgn0037050
Ilk	Integrin linked kinase	Ilk-RA	CG10504	FBgn0028427
Imp	IGF-II mRNA-binding protein	Imp-RA	CG1691	FBgn0285926
Jra	Jun-related antigen	Jra-RA	CG2275	FBgn0001291
Klp61F	Kinesin-like protein at 61F	Klp61F-RA	CG9191	FBgn0004378
krz	kurtz	krz-RA	CG1487	FBgn0040206
LamC	Lamin C	LamC-RA	CG10119	FBgn0010397
lid	little imaginal discs	lid-RA	CG9088	FBgn0031759
Liprin-alpha	Liprin-alpha	Liprin-alpha-RA	CG11199	FBgn0046704
Lis-1	Lissencephaly-1	Lis-1-RA	CG8440	FBgn0015754
Lmpt	Limpet	Lmpt-RA	CG42679	FBgn0261565
loqs	loquacious	loqs-RB	CG6866	FBgn0032515
Mad	Mothers against dpp	Mad-RA	CG12399	FBgn0011648
Mbs	Myosin binding subunit	Mbs-RE	CG32156	FBgn0005536
metro	menage a trois	metro-RB	CG30021	FBgn0050021
mew	multiple edematous wings	mew-RA	CG1771	FBgn0004456
Mkk4	MAP kinase kinase 4	Mkk4-RA	CG9738	FBgn0024326
MRG15	MORF-related gene 15	MRG15-RA	CG6363	FBgn0027378
mRpL40	ıitochondrial ribosomal protein L4	mRpL40-RA	CG5242	FBgn0037892
mts	microtubule star	mts-RA	CG7109	FBgn0004177
mys	myospheroid	mys-RA	CG1560	FBgn0004657
Nedd4	Nedd4	Nedd4-RK	CG42279	FBgn0259174
Nf-YA	Nuclear factor Y-box A	Nf-YA-RA	CG3891	FBgn0035993
Nf-YC	Nuclear factor Y-box C	Nf-YC-RA	CG3075	FBgn0029905
Nmt	N-myristoyl transferase	Nmt-RA	CG7436	FBgn0020392
nSyb	neuronal Synaptobrevin	nSyb-RA	CG17248	FBgn0013342
nudE	nudE	nudE-RA	CG8104	FBgn0036059
Oat	ıithine aminotransferase precurs	Oat-RA	CG8782	FBgn0022774
Osbp	Oxysterol binding protein	Osbp-RA	CG6708	FBgn0020626
p130CAS	p130CAS	p130CAS-RB	CG1212	FBgn0035101
p38b	p38b MAP kinase	p38b-RA	CG7393	FBgn0024846
p53	p53	p53-RA	CG33336	FBgn0039044
p53	p53	p53-RB	CG33336	FBgn0039044

Pak3	Pak3	Pak3-RA	CG14895	FBgn0044826
par-6	par-6	par-6-RA	CG5884	FBgn0026192
Parp	Poly-(ADP-ribose) polymerase	Parp-RB	CG40411	FBgn0010247
parvin	parvin	parvin-RA	CG32528	FBgn0052528
Pde1c	Phosphodiesterase 1c	Pde1c-RC	CG44007	FBgn0264815
Pdk1	ıosphoinositide-dependent kinase	Pdk1-RA	CG1210	FBgn0020386
Pdp1	PAR-domain protein 1	Pdp1-RB	CG17888	FBgn0016694
Pect	phoethanolamine cytidylyltransfe	Pect-RD	CG5547	FBgn0032482
Pepck2	osphoenolpyruvate carboxykinas	Pepck2-RA	CG10924	FBgn0034356
Pex13	Peroxin 13	Pex13-RA	CG4663	FBgn0033812
Pgm1	Phosphoglucose mutase 1	Pgm1-RA	CG5165	FBgn0003076
PHGPx	PHGPx	PHGPx-RC	CG12013	FBgn0035438
PhKgamma	Phosphorylase kinase gamma	PhKgamma-RB	CG1830	FBgn0011754
Pi3K92E	Pi3K92E	Pi3K92E-RA	CG4141	FBgn0015279
PIG-A	lylinositol glycan anchor biosynth	PIG-A-RA	CG6401	FBgn0034270
Pitslre	Pitslre	Pitslre-RA	CG4268	FBgn0016696
Pka-C1	nase, cAMP-dependent, catalytic	Pka-C1-RB	CG4379	FBgn0000273
Pka-R1	e, cAMP-dependent, regulatory s	Pka-R1-RK	CG42341	FBgn0259243
Pka-R2	e, cAMP-dependent, regulatory s	Pka-R2-RA	CG15862	FBgn0022382
Pkg21D	tein kinase, cGMP-dependent at	Pkg21D-RA	CG3324	FBgn0000442
Pnn	Pinin	Pnn-RA	CG8383	FBgn0037737
Pp1-13C	Protein phosphatase 1 at 13C	Pp1-13C-RA	CG9156	FBgn0003132
Pp1alpha-96A	rotein phosphatase 1alpha at 96	Pp1alpha-96A-RA	CG6593	FBgn0003134
Pp4-19C	Protein phosphatase 19C	Pp4-19C-RA	CG32505	FBgn0023177
prd	paired	prd-RA	CG6716	FBgn0003145
primo-2	primo-2	primo-2-RB	CG33747	FBgn0040076
Psn	Presenilin	Psn-RA	CG18803	FBgn0284421
PSR	phosphatidylserine receptor	PSR-RA	CG5383	FBgn0038948
Ptp61F	Protein tyrosine phosphatase 61F	Ptp61F-RC	CG9181	FBgn0267487
Pu	Punch	Pu-RA	CG9441	FBgn0003162
Rab10	Rab10	Rab10-RA	CG17060	FBgn0015789
Rab11	Rab11	Rab11-RA	CG5771	FBgn0015790
Rab18	Rab18	Rab18-RA	CG3129	FBgn0015794
Rab2	Rab2	Rab2-RA	CG3269	FBgn0014009
Rab21	Rab21	Rab21-RA	CG17515	FBgn0039966
Rab23	Rab23	Rab23-RA	CG2108	FBgn0037364
Rab3	Rab3	Rab3-RA	CG7576	FBgn0005586
Rab30	Rab30	Rab30-RA	CG9100	FBgn0031882
Rab32	Rab32	Rab32-RC	CG8024	FBgn0002567
Rab35	Rab35	Rab35-RA	CG9575	FBgn0031090
Rab5	Rab5	Rab5-RA	CG3664	FBgn0014010

Rab6	Rab6	Rab6-RA	CG6601	FBgn0015797
Rab7	Rab7	Rab7-RA	CG5915	FBgn0015795
Rab8	Rab8	Rab8-RA	CG8287	FBgn0262518
Rab9	Rab9	Rab9-RA	CG9994	FBgn0032782
Rab9Fb	Rab at 9Fb	Rab9Fb-RA	CG32670	FBgn0052670
RabX1	RabX1	RabX1-RA	CG3870	FBgn0015372
RabX6	RabX6	RabX6-RA	CG12015	FBgn0035155
Rac1	Rac1	Rac1-RA	CG2248	FBgn0010333
Rac2	Rac2	Rac2-RA	CG8556	FBgn0014011
Rack1	eptor of activated protein kinase	Rack1-RA	CG7111	FBgn0020618
Raf	Raf oncogene	Raf-RA	CG2845	FBgn0003079
Rala	Ras-like protein A	Rala-RA	CG2849	FBgn0015286
Ran	Ran	Ran-RA	CG1404	FBgn0020255
Rap1	Rap1 GTPase	Rap1-RA	CG1956	FBgn0004636
Rap2l	Ras-associated protein 2-like	Rap2l-RA	CG3204	FBgn0283666
ras	raspberry	ras-RB	CG1799	FBgn0003204
Ras64B	Ras oncogene at 64B	Ras64B-RA	CG1167	FBgn0003206
Rel	Relish	Rel-RA	CG11992	FBgn0014018
Rho1	Rho1	Rho1-RA	CG8416	FBgn0014020
RhoGAP5A	ho GTPase activating protein at 5	RhoGAP5A-RB	CG3208	FBgn0029778
RhoGDI	RhoGDI	RhoGDI-RA	CG7823	FBgn0036921
RnrS	oside diphosphate reductase sma	RnrS-RA	CG8975	FBgn0011704
RpL10	Ribosomal protein L10	RpL10-RC	CG17521	FBgn0024733
RpL13A	Ribosomal protein L13A	RpL13A-RB	CG1475	FBgn0037351
RpL40	Ribosomal protein L40	RpL40-RA	CG2960	FBgn0003941
RpS6	Ribosomal protein S6	RpS6-RA	CG10944	FBgn0261592
rush	rush hour	rush-RA	CG14782	FBgn0025381
Sam-S	S-adenosylmethionine Synthetase	Sam-S-RA	CG2674	FBgn0005278
scramb1	scramblase 1	scramb1-RA	CG32056	FBgn0052056
sgg	shaggy	sgg-RB	CG2621	FBgn0003371
sgl	sugarless	sgl-RA	CG10072	FBgn0261445
shtd	shattered	shtd	CCG9198	FBgn0004391
sina	seven in absentia	sina-RA	CG9949	FBgn0003410
Sk1	Sphingosine kinase 1	Sk1-RA	CG1747	FBgn0030300
Skp2	-phase kinase-associated protein	Skp2	CG9772	FBgn0037236
SkpB	SKP1-related B	SkpB-RA	CG8881	FBgn0026176
slmb	supernumerary limbs	slmb-RA	CG3412	FBgn0283468
Smox	Smad on X	Smox-RA	CG2262	FBgn0025800
sn	singed	sn-RA	CG32858	FBgn0003447
Sod2	Superoxide dismutase 2 (Mn)	Sod2-RA	CG8905	FBgn0010213
Spps	ke factor for pairing sensitive-sile	Spps-RA	CG5669	FBgn0039169

Sptr	Sepiapterin reductase	Sptr-RA	CG12117	FBgn0014032
sqa	spaghetti-squash activator	sqa-RB	CG42347	FBgn0259678
sqh	spaghetti squash	sqh-RA	CG3595	FBgn0003514
Src64B	Src oncogene at 64B	Src64B-RC	CG7524	FBgn0262733
SREBP	ol regulatory element binding prc	SREBP-RA	CG8522	FBgn0261283
STUB1	omology and U-box containing pı	STUB1-RA	CG5203	FBgn0027052
Su(var)2-10	Suppressor of variegation 2-10	Su(var)2-10-RD	CG8068	FBgn0003612
Su(var)2-10	Suppressor of variegation 2-10	Su(var)2-10-RF	CG8068	FBgn0003612
Su(var)3-3	Suppressor of variegation 3-3	Su(var)3-3-RA	CG17149	FBgn0260397
Su(z)12	Su(z)12	Su(z)12-RA	CG8013	FBgn0020887
Swip-1	Swiprosin-1	Swip-1-RA	CG10641	FBgn0032731
Syb	Synaptobrevin	Syb-RA	CG12210	FBgn0003660
Synd	Syndapin	Synd-RB	CG33094	FBgn0053094
Syx1A	Syntaxin 1A	Syx1A-RA	CG31136	FBgn0013343
Tace	Tace	Tace-RA	CG7908	FBgn0039734
Tak1	TGF-β activated kinase 1	Tak1-RA	CG18492	FBgn0026323
Tango4	Transport and Golgi organization 4	Tango4-RA	CG1796	FBgn0030365
Taz	Tafazzin	Taz-RA	CG8766	FBgn0026619
TBCB	tubulin-binding cofactor B	TBCB-RA	CG11242	FBgn0034451
Tbp	TATA binding protein	Tbp-RA	CG9874	FBgn0003687
Tcs3	Tcs3	Tcs3-RA	CG4933	FBgn0283681
TfAP-2	Transcription factor AP-2	TfAP-2-RB	CG7807	FBgn0261953
Tfb1	Transcription factor B1	Tfb1-RA	CG8151	FBgn0033929
Tg	Transglutaminase	Tg-RA	CG7356	FBgn0031975
Tip60	Tat interactive protein 60kDa	Tip60-RA	CG6121	FBgn0026080
tmod	tropomodulin	tmod-RB	CG1539	FBgn0082582
Traf4	TNF-receptor-associated factor 4	Traf4-RA	CG3048	FBgn0026319
Traf6	TNF-receptor-associated factor 6	Traf6-RA	CG10961	FBgn0265464
Tsc1	Tsc1	Tsc1-RA	CG6147	FBgn0026317
Tsp66E	Tetraspanin 66E	Tsp66E-RA	CG4999	FBgn0035936
Tsp96F	Tetraspanin 96F	Tsp96F-RA	CG6120	FBgn0027865
Ubc10	Ubiquitin conjugating enzyme 10	Ubc10-RA	CG5788	FBgn0026316
Ube3a	Ubiquitin protein ligase E3A	Ube3a-RA	CG6190	FBgn0061469
Ufd1-like	Ubiquitin fusion-degradation 1-lik	Ufd1-like-RA	CG6233	FBgn0036136
Uros1	Uroporphyrinogen III synthase 1	CG1885-RA	CG1885	FBgn0030066
usp	ultraspiracle	usp-RA	CG4380	FBgn0003964
Vav	guanine nucleotide exchange fac	Vav-RA	CG7893	FBgn0040068
Vinc	Vinculin	Vinc-RA	CG3299	FBgn0004397
Vps28	Vacuolar protein sorting 28	Vps28-RA	CG12770	FBgn0021814
WASp	WASp	WASp-RA	CG1520	FBgn0024273
wbl	windbeutel	wbl-RA	CG7225	FBgn0004003

Wdfy2	repeat and FYVE domain containi	Wdfy2-RA	CG5168	FBgn0032246
Wwox	V domain containing oxidoreduct	Wwox-RA	CG7221	FBgn0031972
zda	zonda	zda-RA	CG5482	FBgn0034368

*peptide no longer matches FlyBase annotation

CDS size	Gold Source Clone	Accession number	Donor clone stop (DS)	DS Accession number	GFP::ORF	RFP::ORF
1128	LD18090	AY118907	BS15418	KX801817	UGS01407	URS01407
1128	RE02927	AY089562	BS11334	FJ636827	UGS01271	URS01271
2685	LD37956	AY069615	ND	~		
1035	GH14845	AY060709	BS09556	FJ638826	UGS01220	URS01220
3978	LD21322	AY061300	BS11048	KX802002	UGS01492	URS01492
1029	LD44987	AY118588	BS08872	MN238604	UGS01215	
2508	LD25543	AY069534	ND	~		
1122	LD23542	AY051685	BS06802	FJ635621	UGS01372	URS01372
1962	GH12584	AY119509	ND	~		
972	LD09947	AY118504	BS04048	FJ634842	UGS01331	URS01331
585	RE25242	AY071207	BS11859	FJ636999	UGS01487	URS01487
1470	GH14842	AY051495	BS07363	FJ635831	UGS01385	URS01385
1449	RH26053	BT001795	BS15971	FJ638001	UGS01415	
2661	GH04413	AF181628	ND	~		
525	RE16882	AY071116	ND	~		
546	LD24904	AY060375	BS05649	FJ635191	UGS01351	URS01351
1656	LD46935	AY069700	BS10163	KX804690	UGS01257	URS01257
1182	LD18955	AY061256	BS04230	FJ634886	UGS01357	URS01357
1254	LD35711	AY051859	BS08482	FJ638812	UGS01204	URS01204
903	LD29815	AY060391	BS08078	FJ636093	UGS01202	URS01202
522	SD24339	AY119268	BS15269	FJ637907	UGS01472	URS01472
453	RH48239	AY089678	BS13858	FJ637540	UGS01256	URS01256
1431	LD23642	AY051688	BS17605	KX800222	UGS01423	URS01423
1452	LD33682	BT001498	BS17738	KX800750	UGS01435	URS01435
363	LD05816	AY122152	BS03649	FJ638771	UGS01328	URS01328
729	RE36486	BT011453	BS16081	FJ638055	UGS01478	URS01478
1515	RE10864	AY118367	BS11538	FJ636899	UGS01430	URS01430
471	RE24457	AY071203	BS11948	FJ637029	UGS01463	URS01463
297	RE20862	AY071165	BS11796	FJ636975	UGS01279	URS01279
891	RE35715	AY113454	BS12071	FJ637060	UGS01282	URS01282
627	GH01760	AY058261	BS06972	FJ635679	UGS01378	URS01378
1797	LD09009	AF160917	BS03617	FJ634726	UGS01237	URS01237
1341	LD43681	BT003242	BS15123	KX806269	UGS01406	URS01406
1338	GH02051	AY118725	BS14906	FJ637829	UGS01404	
1656	HL08087	BT003592	BS10401	FJ636639	UGS01228	URS01228
1641	RE01910	AY094843	BS11320	FJ636821	UGS01269	URS01269
1812	LD29068	AY051758	BS08061	FJ636084	UGS01247	URS01247
1347	RE17834	AY095071	BS11757	FJ636960	UGS01315	URS01315

1116	HL02677	AY070865	BS04602	FJ634972	UGS01339	URS01339
2358	LD16208	AY128441	BS05076	KX795404		URS01443
897	AT16536	AY075219	BS14274	FJ637627	UGS01295	URS01295
1500	LD10168	AY069399	BS01549	FJ634644	UGS01317	URS01317
1866	RE54552	AY128480	BS12368	KX805643	UGS01468	URS01468
1599	GH13725	AY051470	BS07223	FJ635773	UGS01242	URS01242
2034	LD09850	BT010078	BS05017	KX794414		URS01442
2700	LD12661	BT021947	BS15481	KX801947	UGS01473	URS01473
573	HL08128	AY119570	BS03306	FJ634713		
1725	LD35753	AY051861	BS08484	FJ636179	UGS01251	URS01251
891	LD38718	AY061450	BS06587	FJ635552	UGS01365	URS01365
2454	GH10652	AY102660	ND	~		
561	GH28351	AY113352	BS14872	FJ637815	UGS01471	URS01471
1068	LD22010	AY118916	BS05610	FJ635161	UGS01350	URS01350
1473	SD03973	AY052088	BS09340	FJ636400	UGS01219	URS01219
684	LP10861	AY069750	BS06288	FJ635432	UGS01360	URS01360
2619	GH02025	AY058267	BS07277	FJ635800	UGS01243	URS01243
1818	GH22690	AY051576	BS07690	FJ635951	UGS01246	URS01246
450	RH49748	AY071745	BS13964	FJ637568	UGS01292	URS01292
1809	RE33807	AY071312	BS12053	KX804479	UGS01464	
1011	LD10183	AY069400	BS04050	FJ634844	UGS01332	URS01332
1860	RE18568	AY095527	BS11775	KX805359	UGS01462	URS01462
1629	GH05942	AY058297	BS07113	FJ635733	UGS01382	URS01382
1134	AT31332	AY075301	BS12731	FJ637281	UGS01401	URS01401
1194	RE02540	BT021331	BS16738	FJ638186	UGS01434	URS01434
462	AT19555	AY070806	BS12785	FJ637292	UGS01403	URS01403
1317	GH19141	AY051542	BS07744	MN238600	UGS01388	URS01388
1833	LD02975	AY061059	BS03015	FJ634690	UGS01239	URS01239
5034	LD43101	AY119615	BS11028	KX802159	UGS01486	URS01486
1803	GH09380	AY069078.1	ND	~		
2190	LD41760	AY061460	ND	~		
645	RE31047	AY113447	BS12026	FJ637039	UGS01281	URS01281
1677	LD29964	AY051774	BS08083	MN238597	UGS01248	URS01248
528	AT07685	AY084105	BS13760	FJ637521	UGS01293	URS01293
813	RE60886	BT012456	BS16314	FJ638116		URS01418
1830	LD07634	AY122153	BS15459	KX803675	UGS01408	URS01408
2523	LD22829	BT001484	BS03210	FJ634694	UGS01235	URS01235
1020	GH06546	AY060640	BS07022	FJ635692	UGS01383	URS01383
1473	LD44443	AY058712	BS08955	FJ636323	UGS01212	URS01212
801	LD35705	AY061425	BS06196	FJ635392	UGS01358	URS01358
1431	LD22957	AY069509	BS06692	FJ635590		URS01371

1698	LD46284	AY058720	BS10622	FJ636696		URS01429
1494	LD34777	AY051844	BS08565	FJ636199		URS01203
564	GH09983	AY060670	BS06523	FJ635531	UGS01362	
2028	LD18186	AY095032	BS04649	KX794325		URS01441
1644	LD42588	AY119614	BS08921	FJ636318	UGS01209	URS01209
633	LD12029	AY061142	BS02810	FJ634676	UGS01238	URS01238
1188	LD41207	AY058692	BS08685	FJ636235	UGS01252	
1155	GM02110	AY060841	BS04728	FJ635017	UGS01341	URS01341
2280	LD30505	AY051785	BS01296	FJ634590	UGS01322	URS01322
1116	GH09856*	AY069083	BS16823	KX805932	UGS01421	URS01421
1170	RE54950	AY071474	BS12277	FJ637130	UGS01326	URS01326
744	RE36735	BT012467	BS16311	FJ638114	UGS01417	URS01417
1428	LD19162	AY061261	BS04234	FJ634887	UGS01333	URS01333
1128	LD03509	AY061065	BS03889	FJ634814	UGS01305	URS01305
843	GH01314	AY058251	BS06964	FJ635675	UGS01377	URS01377
678	SD11336	BT001878	BS17974	KX803751	UGS01426	URS01426
1278	SD10657	AY058794	BS09502	FJ636432		URS01447
1068	LP11503	AY069755	BS09979	FJ636515	UGS01223	URS01223
1275	RE74011	BT009962	BS16376	MN238598		URS01431
1383	GH05039	AY069047	BS07406	FJ635845		URS01494
993	LD26412	AY118534	BS06620	MN238602	UGS01366	URS01366
1434	GH07620	BT001403	BS15605	KX802445	UGS01411	URS01411
1530	HL02049	AY089526	BS05072	FJ635055	UGS01344	URS01344
1065	LD22201	AY051670	BS06675	FJ635585	UGS01370	URS01370
1062	GM01620	AY121631	BS04626	MN238599		URS01340
1155	LD26182	AY058572	BS10509	FJ636687		URS01229
2649	RE37840	BT001628	BS14096	KX800981	UGS01233	URS01233
1020	LD25526	AY058566	BS08015	FJ636059	UGS01394	
1074	RH17413	BT004841	BS13476	FJ638854	UGS01289	URS01289
1329	LP03430	BT003563	ND	~		
414	RE40543	BT014645	BS16196	KX803490	UGS01477	URS01477
2361	LD23641	AY075384	BS10205	FJ636594	UGS01485	URS01485
1458	RE40104	AY071369	BS01543	FJ634641	UGS01309	URS01309
1347	RE64348	AY071593	BS01528	FJ634634	UGS01321	URS01321
837	LD34464	AY119609	BS10149	FJ636575	UGS01224	URS01224
999	RE02181	AY121654	BS11324	FJ636822	UGS01270	URS01270
1011	RE40955	AY119633	BS01472	FJ634621	UGS01303	URS01303
1563	GM14158	AY058487	BS06640	FJ635573	UGS01368	URS01368
1314	LD23745	AY061321	BS06812	FJ635628	UGS01373	URS01373
3384	LD43531	BT004866	BS10704	KX801354	UGS01455	URS01455
1362	RH33703	AY071719	BS13820	KX802974	UGS01291	URS01291

1395	LD26976	AY051743	BS08035	FJ636068	UGS01201	URS01201
2112	RE09535	BT003533	BS01601	FJ634654		URS01311
882	GH03058	AY047523	BS07387	FJ635837	UGS01386	URS01386
1140	GH11957	BT012317	BS16504	FJ638153	UGS01419	URS01419
2169	GH14435	AY051486	BS01285	FJ634586	UGS01319	URS01319
1155	LD32727	BT012315	BS16432	FJ638145	UGS01420	URS01420
1266	AT14262	AY075206	BS14251	KX805345	UGS01294	URS01294
615	LD47783	BT014655	BS16517	FJ638156	UGS01493	URS01493
1233	GH23156	AY051584	BS07804	FJ635992	UGS01389	URS01389
1344	LD24671	AY051708	BS06840	FJ635639	UGS01375	URS01375
1698	SD07045	AY069821	ND	~		
867	LD25202	AY058562	BS01052	FJ634511	UGS01302	URS01302
3198	LD15641	AY069442	BS04093	KX794262	UGS01440	URS01440
1410	LD31082	AY118946	BS03268	FJ634709	UGS01439	URS01439
1863	LD31805	AY095046	BS08414	FJ636146	UGS01250	URS01250
5514	LD40310	AY095051	ND	~		
3603	LD33094	BT004484	ND	~		
1233	LD11219	BT021404	BS15473	KX800932	UGS01409	URS01409
735	RE22626	AY128470	BS16687	FJ638182	UGS01482	URS01482
1395	RE14437	AY071070	BS11495	FJ636889	UGS01275	URS01275
1365	RE72705	BT004845	BS01529	FJ634635	UGS01316	URS01316
1131	GH16214	AY051508	BS07493	FJ635888	UGS01445	URS01445
1668	GH12103	BT003617	BS09540	FJ636440	UGS01448	URS01448
3147	GH14509	AY075338	BS10262	FJ636620	UGS01258	URS01258
1272	RE70055	AY070600	BS02838	FJ634684	UGS01232	URS01232
1272	LD22902	AY051679	BS07991	FJ636052	UGS01393	URS01393
588	RE65766	AY071609	BS13216	FJ637392	UGS01287	URS01287
927	LD26077	AY058571	BS08023	FJ636063	UGS01396	URS01396
2538	RE55238	AY113499	BS13064	KX806112	UGS01488	URS01488
2502	SD04682	AY061595	ND	~		
1197	LD21748	AY118913	BS01111	FJ634532		URS01307
1803	RE43755	BT001649	BS01577	MN238603	UGS01310	URS01310
1416	GM13220	AF132556	BS05308	FJ635094		URS01345
549	GH04664	AY069045	BS05672	FJ635210		URS01354
951	LD19982	AY061280	BS04240	FJ634892	UGS01334	URS01334
1293	GH01984	AY047517	BS06883	FJ635656	UGS01379	URS01379
2352	LD31802	AY129448	ND	~		
1704	GH02705	AY058273	BS07383	FJ635836	UGS01244	URS01244
1095	LD24658	AY058548	BS03211	FJ634695	UGS01241	URS01241
1155	GH11591	AY069096	BS01103	FJ634528	UGS01306	URS01306
1485	AT28346	BT001357	BS12663	FJ637258	UGS01402	URS01402

1707	LD10376	BT003278	BS15422	KX805222	UGS01489	
1053	LD29223	AY061369	BS10184	FJ636586	UGS01227	URS01227
2982	RE04933	BT015238	BS16644	KX800772	UGS01481	URS01481
1101	GH23568	BT016127	BS16867	FJ638204	UGS01422	URS01422
1815	RE56844	AY118396	ND	~		
2265	LD22131	BT004489	ND	~		
810	GM02880	BT003290	ND	~		
1143	RE62261	BT003190	BS15893	KX803964	UGS01416	URS01416
1914	RE12569	AY094852	BS11463	KX803442	UGS01460	URS01460
1320	RE69884	BT001726	BS15848	KX801458	UGS01414	URS01414
1680	LD36183	BT010043	BS10152	KX803110	UGS01225	URS01225
594	SD18370	BT011331	BS15670	KX805987	UGS01412	URS01412
1257	GH28523	AY051635	BS07875	FJ636017	UGS01392	URS01392
3264	SD05105	BT003173	ND	~		
1437	LD44262	AY122191	BS08852	FJ636299	UGS01211	URS01211
2856	LD39519	BT016092	BS17648	KX802158	UGS01436	URS01436
1059	LD13640	AY069425	BS04669	FJ634999	UGS01342	URS01342
1128	LD43873	AY058709	BS08844	FJ636295		URS01210
1131	LD44591	AY069669	BS10160	FJ636578		URS01484
2304	GH03852	AY058288	BS07293	FJ635807	UGS01245	URS01245
909	RE29832	AY071261	BS12114	FJ637073		URS01280
906	GH10637	AY060272	BS07539	FJ635898	UGS01387	URS01387
981	LD14639	BT016110	BS15495	KX804433	UGS01410	URS01410
921	RE58406	AY113503	BS12834	FJ637310	UGS01286	URS01286
1770	GH22686	AY059447	BS01815	FJ634662		URS01320
492	AT28881	AY089477	BS12705	FJ637275	UGS01296	URS01296
1623	LD23505	AY061316	BS17604	KX805486	UGS01483	URS01483
1224	LD25827	AY051727	BS08117	FJ636103	UGS01395	URS01395
1590	LP01280	AY069713	BS09158	FJ636363	UGS01255	URS01255
972	LD37787	AY051890	BS17746	KX801950	UGS01424	URS01424
612	LD39986	AY060425	BS08757	FJ636257	UGS01446	URS01446
642	GM06568	AY070528	BS04282	FJ634913	UGS01335	URS01335
591	GH11193	AY075329	BS05820	FJ635243	UGS01355	URS01355
639	GH01619	BT003315	BS06407	FJ635478	UGS01361	URS01361
567	RE42508	AY119634	BS12457	FJ637190	UGS01285	URS01285
804	RH23273	AY113574	BS13489	FJ637477		URS01290
660	LP05860	AY060449	BS10637	FJ636698	UGS01454	
669	RE14786	AY071080	BS11707	FJ636934	UGS01276	URS01276
1164	LD04613	AY069328	BS04004	FJ634827	UGS01330	URS01330
603	LD21953	AY094795	BS06671	FJ635584	UGS01369	URS01369
657	GH24702	AY060343	BS07832	FJ636005	UGS01391	URS01391

624	GH09086	AY060261	BS07047	FJ635703	UGS01384	URS01384
621	GH03685	AY060236	BS06991	FJ635684	UGS01380	URS01380
621	LD44762	AY069671	BS08961	FJ636326	UGS01214	URS01214
768	RE17845	AY071139	BS11759	FJ638836	UGS01278	URS01278
642	IP08727	BT024998	BS14580	FJ637714	UGS01427	URS01427
783	LD47384	AY122200	BS09126	FJ636357	UGS01217	URS01217
639	RE70650	AY071647	BS13079	FJ637379	UGS01469	URS01469
576	LD34217	AY060408	BS08459	FJ636168	UGS01438	URS01438
576	GM13874	AY118845	BS05469	FJ635129	UGS01346	URS01346
954	RE74715	AY071661	BS02841	FJ634686		URS01288
2217	GH03557	AY089490	BS10234	FJ636610	UGS01490	URS01490
603	LD21679	AY118912	BS05602	FJ635155	UGS01349	URS01349
648	GM14354	AY070533	BS05574	FJ635152	UGS01348	URS01348
552	RE42418	AY121688	BS12554	FJ637216	UGS01284	URS01284
546	RE63021	BT012453	BS16093	FJ638061	UGS01476	URS01476
1611	LD36080	AY089553	BS09916	FJ636505	UGS01495	
576	RE36103	AY119135	BS12173	FJ637087	UGS01465	URS01465
2913	GH01881	AY058264	BS01336	FJ634600	UGS01313	URS01313
576	GH20776	AY119536	BS06543	FJ635537	UGS01364	URS01364
1320	SD02309	AY050239	BS09319	FJ636393	UGS01218	URS01218
603	LD16419	AY061221	BS04210	FJ634878	UGS01337	URS01337
1179	LD41588	AY051936	BS08802	FJ636270	UGS01207	URS01207
654	RE02339	AY070910	BS16737	FJ638185	UGS01433	URS01433
615	GM13948	AY051640	BS05471	FJ635131	UGS01347	URS01347
384	RE10554	AY075451	BS11434	FJ636865	UGS01272	URS01272
651	LD31286	AY058620	BS10439	FJ636661	UGS01230	URS01230
948	GH19261	BT003610	BS14948	FJ637837	UGS01405	
1224	LD40460	AY051918	BS08669	FJ636229	UGS01428	URS01428
1248	GM13876	AY058486	BS06639	FJ635572		URS01367
1542	LD44595	AY122193	BS08958	FJ636324	UGS01213	URS01213
1428	SD09476	AY052137	BS09382	FJ636406	UGS01236	URS01236
492	LD37115*	AY051879	BS08610	FJ636207	UGS01206	URS01206
942	HL08111	AY060358	BS06645	FJ635576	UGS01254	
1923	RE64552	AY119652	BS13207	KX805712	UGS01467	
945	GM13370*	AY060981	BS09612	FJ636452	UGS01221	URS01221
483	IP02725	BT023253	BS17067	FJ638243	UGS01479	URS01479
1530	LD08669	AY118898	BS05002	FJ635028	UGS01240	URS01240
1458	LD15813	BT016105	ND	~		
1536	RH62992	AY071759	BS14010	KX805777	UGS01470	URS01470
651	GH02759	BT004505	BS05651	FJ635193	UGS01352	URS01352
2904	LD04007	AY089533	BS01623	FJ638767	UGS01323	URS01323

783	GH04031	AY118731	BS05664	FJ635204	UGS01353	
1338	GH17420	AY060726	BS09464	FJ636424	UGS01449	URS01449
522	LD14743	AY122159	BS02803	FJ634675	UGS01231	URS01231
1656	LD30429	AY051781	ND	~		
3339	LP12374	BT010285	BS01347	FJ634604	UGS01314	
867	RE01069	AY069760	BS11302	FJ636812	UGS01268	URS01268
1803	RE73180	BT001740	BS15854	KX805206	UGS01474	URS01474
1599	RE55465	BT021257	BS18055	KX804603	UGS01437	URS01437
2670	LD45081	AY094837	BS10614	KX801710	UGS01264	URS01264
2565	SD04959	AY069809	ND	~		
651	SD04693	AY094963	BS10177	FJ636584	UGS01226	URS01226
387	SD05285	BT009942	BS17965	KX803730	UGS01425	URS01425
1482	LD46328	AY069690	BS08894	FJ636315		URS01216
873	LD43943	AY061472	BS09946	FJ636509	UGS01222	URS01222
2196	RE65757	BT003184	BS15937	KX800618	UGS01413	URS01413
2034	LD42274	AY051953	BS08818	FJ636277	UGS01253	URS01253
1446	LD24662	AY051707	BS06939	FJ635671		URS01374
1134	RE14108	AY071059	BS11482	FJ636886	UGS01274	URS01274
732	LD45244	AY061489	BS06240	FJ635409	UGS01359	URS01359
1059	LD44083	AY069663	BS01082	FJ634519	UGS01304	URS01304
1041	RE13621	AY094853	BS11472	FJ636882	UGS01273	URS01273
1395	RE17884	AY071140	BS01533	FJ634637	UGS01308	URS01308
1755	SD04652	AY052097	ND	~		
2328	RE08173	BT010024	BS16278	KX804384		URS01432
1623	LD31064	AY051795	BS08505	FJ636186	UGS01249	URS01249
1209	GH23271	AY094727	BS07805	FJ635993	UGS01390	URS01390
1458	LD20987	AY094792	BS04254	FJ634901	UGS01338	URS01338
1425	GH01161	AY047501	BS06959	FJ635674	UGS01376	
3300	LD23779	AY118330	BS10207	FJ636595		URS01451
801	RE39068	AY118391	BS12411	FJ637162	UGS01283	URS01283
804	LD19727	AF160941	BS03726	FJ634761	UGS01327	URS01327
462	RE47264	BT012459	BS16091	FJ638060	UGS01475	URS01475
2919	LD21888	AY069489	BS10855	KX800269	UGS01459	URS01459
948	GH18603	AY060735	BS06101	FJ635351	UGS01356	URS01356
831	GH17465	AY060729	BS06537	FJ635534	UGS01363	URS01363
1524	LD09973	AY069393	BS02253	FJ634666	UGS01343	URS01343
2379	LD25754	AY069536	BS10816	KX804777	UGS01456	URS01456
2883	SD03117	AY128501	BS10843	KX801314	UGS01457	URS01457
630	GH04443	AY060620	BS06895	FJ635661	UGS01381	URS01381
1581	RE12101	AY070576	BS11456	FJ636874	UGS01461	URS01461
771	IP02648	BT023269	BS17164	FJ638261	UGS01480	

1224	LD41958	AY051942	BS08807	FJ636272	UGS01208	URS01208
1227	LD03827	AY119574	BS03994	FJ634824	UGS01329	
1191	LD36412	AY058659	BS08591	FJ636203		URS01205

Donor clone open (DO)	DO Accession number	ORF::GFP	ORF::RFP	4-way	2-way	FRET
BO15418	FJ633451	UGO01207	URO01207	yes	yes	
BO11734	FJ632172	UGO01171	URO01171	yes	yes	
BO10969	FJ631941	UGO01162				
BO09856	FJ631595		URO01120		yes	
BO11448	KX798731	UGO01292	URO01292	yes	yes	
BO09372	FJ631486	UGO01322	URO01115		yes	
BO10808	FJ631880	UGO01331				
BO07302	FJ630741		URO01072		yes	
BO11081	FJ631990	UGO01167	URO01167		yes	
BO04448	FJ629768	UGO01031	URO01031	yes	yes	
BO12359	FJ632414	UGO01287	URO01287	yes	yes	
BO07663	FJ630884		URO01085		yes	
BO15771	FJ633577	UGO01215	URO01215		yes	
BO05646	FJ630114	UGO01244	URO01244		yes	
BO12040	FJ632290	UGO01177	URO01177		yes	
BO06049	FJ630253	UGO01051	URO01051	yes	yes	
ND	~				yes	
BO04730	FJ629855		URO01057		yes	
BO08882	FJ631300	UGO01104			yes	★
BO08578	FJ631245	UGO01102	URO01102	yes	yes	
BO15369	FJ633432	UGO01272	URO01272	yes	yes	
BO13858	FJ632954		URO01156		yes	
BO17805	FJ634222	UGO01223	URO01223	yes	yes	
BO17838	FJ634234	UGO01235	URO01235	yes	yes	
BO04049	FJ629615		URO01028		yes	
BO16181	FJ633728	UGO01278	URO01278	yes	yes	
BO11938	FJ632252	UGO01230	URO01230	yes	yes	
BO12248	FJ632378	UGO01263	URO01263	yes	yes	
BO12196	FJ632354	UGO01179			yes	
BO12571	FJ638703	UGO01182	URO01182	yes	yes	
BO07372	FJ630767	UGO01078	URO01078	yes	yes	
BO04017	FJ629601	UGO01137	URO01336	yes	yes	
BO15123	FJ633349		URO01206		yes	
BO14906	FJ633272	UGO01204	URO01204		yes	
BO10901	FJ631916	UGO01128	URO01128	yes	yes	
BO11720	FJ632167	UGO01169	URO01169	yes	yes	
BO08561	FJ631239	UGO01147	URO01147	yes	yes	
BO03627	FJ629572	UGO01015	URO01306	yes	yes	

BO04802	FJ629865	UGO01309			yes	
BO05476	FJ630057	UGO01243			yes	
BO14674	FJ633221		URO01195		yes	
BO05426	FJ630030		URO01017		yes	
BO13268	FJ632742	UGO01268			yes	
BO07723	FJ630908	UGO01142	URO01142	yes	yes	
BO05417	FJ630024	UGO01242	URO01242		yes	
BO15481	FJ633490	UGO01273			yes	
BO03858	FJ629590	UGO01134	URO01134		yes	★
BO08884	FJ631302	UGO01151	URO01151	yes	yes	
BO06887	FJ630582		URO01065		yes	
BO10625	FJ631819	UGO01252	URO01252		yes	
BO14872	FJ633264		URO01271		yes	
BO06010	FJ630222	UGO01050	URO01050	yes	yes	
BO09740	FJ631561	UGO01119	URO01119	yes	yes	
BO06788	FJ630532	UGO01060	URO01060	yes	yes	
BO07777	FJ630926	UGO01143	URO01143	yes	yes	
BO08190	FJ631095		URO01146		yes	
BO13864	FJ632958	UGO01335	URO01192	yes	yes	
BO12453	FJ632446	UGO01264	URO01264		yes	
BO04450	FJ629770	UGO01032	URO01032	yes	yes	
BO12075	FJ632302	UGO01262	URO01262	yes	yes	
BO07413	FJ630776	UGO01082	URO01082	yes	yes	
BO16231	FJ633742	UGO01201			yes	
BO17738	FJ634197	UGO01234	URO01234	yes	yes	
BO16385	FJ633806	UGO01203	URO01203	yes	yes	
BO08144	FJ631076	UGO01088	URO01088	yes	yes	
BO04976	FJ638626	UGO01139	URO01139	yes	yes	
ND	~				yes	
BO10514	FJ631796	UGO01250	URO01250		yes	
BO10890	FJ631914	UGO01163	URO01163		yes	
BO12526	FJ632472	UGO01181	URO01342	yes	yes	
BO08583	FJ631246		URO01148		yes	
BO14360	FJ633102	UGO01193	URO01193	yes	yes	
BO16414	FJ633820	UGO01218	URO01218		yes	
BO15459	FJ633479	UGO01208	URO01208	yes	yes	
BO03662	FJ629581	UGO01135	URO01135	yes	yes	
BO07422	FJ630780		URO01083		yes	
BO09255	FJ631448	UGO01112			yes	
BO06596	FJ630456	UGO01311	URO01058	yes	yes	
BO07192	FJ630699		URO01071			

BO11122	FJ632004	UGO01229			yes
BO08865	FJ631295	UGO01103			yes
BO06823	FJ630547	UGO01062	URO01062		yes
BO04849	FJ629894	UGO01241	URO01241		yes
BO09221	FJ631433	UGO01109	URO01109	yes	yes
BO04662	FJ629832	UGO01138	URO01138	yes	yes
BO09185	FJ631423	UGO01152	URO01152		yes
BO04828	FJ629880	UGO01041	URO01314	yes	yes
BO01296	FJ629469		URO01022		yes
BO17223	FJ634060	UGO01221	URO01221	yes	yes
BO22320	KX795772	UGO01026	URO01310	yes	yes
BO16511	FJ633847	UGO01217	URO01217	yes	yes
BO04634	FJ629819		URO01033		yes
BO01483	FJ629516	UGO01005	URO01005	yes	yes
BO07364	FJ630761	UGO01317	URO01324	yes	yes
BO18074	FJ634307	UGO01226			yes
BO09902	MN238606	UGO01247	URO01247		yes
BO10379	FJ631727	UGO01123			yes
BO16576	FJ633868	UGO01231			yes
BO21745	KX794432	UGO01294	URO01294		yes
BO07020	FJ630629	UGO01312	URO01066	yes	yes
BO15805	FJ633589	UGO01211	URO01211	yes	yes
BO05472	FJ630054		URO01044		yes
BO07075	FJ630652	UGO01070	URO01320	yes	yes
BO04826	FJ629878	UGO01040	URO01040		yes
BO10909	FJ631920	UGO01129	URO01129		yes
BO03746	FJ629588	UGO01326			yes
BO08515	FJ631223	UGO01094	URO01094		yes
BO13676	FJ632901	UGO01189	URO01344	yes	yes
BO01141	FJ629434	UGO01012	URO01305		yes
BO16096	FJ633718	UGO01277	URO01277	yes	yes
BO10605	KX797345		URO01285		yes
BO02243	FJ629558		URO01303		yes
BO08620	FJ631260		URO01021		yes
BO10449	FJ631763	UGO01124	URO01124	yes	yes
BO11724	FJ632169	UGO01170	URO01170	yes	yes
BO01472	FJ629511	UGO01003	URO01003	yes	yes
BO07140	FJ630683	UGO01068	URO01068	yes	yes
BO07312	FJ630747		URO01321		yes
BO11104	FJ631999	UGO01255			yes
BO13820	FJ632936	UGO01191			yes

BO08535	FJ631228	UGO01101	URO01101	yes	yes
BO01601	FJ629546	UGO01011	URO01011		yes
BO07787	FJ630929	UGO01086	URO01326	yes	yes
BO17004	FJ634008	UGO01219	URO01219	yes	yes
BO07651	FJ630875		URO01309		yes
BO17132	FJ634036	UGO01220	URO01220	yes	yes
BO14651	FJ633215	UGO01194	URO01194	yes	yes
BO17017	KX799624	UGO01293	URO01293	yes	yes
BO08304	FJ631143	UGO01089			yes
BO07240	FJ630718	UGO01316	URO01323	yes	yes
BO11245	FJ632039		URO01258		
BO01052	FJ629404		URO01002		yes
BO04493	FJ629784	UGO01240	URO01240	yes	yes
BO03268	MN238596	UGO01239			yes
BO08814	FJ631280	UGO01150	URO01150	yes	yes
BO11422	KX799863	UGO01304	URO01025		yes
BO10952	FJ631934	UGO01161	URO01338		yes
BO15473	FJ633485	UGO01209	URO01209	yes	yes
BO17687	FJ634191	UGO01282			yes
BO11995	FJ632274	UGO01332	URO01175	yes	yes
BO03940	FJ629594		URO01307		yes
BO07993	FJ631009	UGO01245			yes
BO09940	KX796929	UGO01248	URO01248	yes	yes
BO10662	FJ631832	UGO01330	URO01158	yes	yes
BO03638	FJ629576		URO01132		yes
BO08391	FJ631174	UGO01093	URO01093	yes	yes
BO13116	FJ632680	UGO01334	URO01187	yes	yes
BO08523	FJ631225		URO01096		yes
BO13564	KX799531	UGO01288	URO01288	yes	yes
BO11155	FJ632014	UGO01165	URO01165		yes
BO01112	FJ629425	UGO01007	URO01007		yes
BO01577	FJ629540	UGO01022	URO01304	yes	yes
BO05608	FJ630087	UGO01045	URO01315		yes
BO06072	FJ630271	UGO01054	URO01054		yes
BO04640	FJ629822	UGO01034	URO01034	yes	yes
BO07283	FJ630734		URO01079		yes
BO10842	FJ631892	UGO01160	URO01160		yes
BO07683	FJ630895	UGO01144	URO01144	yes	yes
BO07237	FJ630717	UGO01141	URO01141	yes	yes
BO01104	FJ629422	UGO01006	URO01006	yes	yes
BO16363	FJ633796	UGO01202	URO01202	yes	yes

BO15422	KX798988	UGO01289	URO01289		yes	
BO10484	FJ638675	UGO01325	URO01127	yes	yes	★
BO17644	FJ634187	UGO01281			yes	
BO17367	FJ634094	UGO01222	URO01222	yes	yes	
BO12806	MN238595	UGO01266				
BO10803	FJ631878	UGO01253	URO01253		yes	
BO01446	KX796304	UGO01001	URO01301		yes	
BO15693	FJ633554	UGO01216			yes	
BO11863	FJ632223	UGO01260	URO01260	yes	yes	
BO15748	FJ633572	UGO01214	URO01214	yes	yes	
BO10452	FJ631766		URO01332		yes	
BO15870	FJ633613	UGO01212	URO01212	yes	yes	
BO08375	FJ631170		URO01092		yes	
BO22128	KX799357		URO01296			
BO09252	FJ631446		URO01111		yes	
BO17948	FJ634262	UGO01236	URO01236	yes	yes	
BO04869	FJ629905	UGO01042	URO01042	yes	yes	
BO09244	FJ631442		URO01110			
BO10560	FJ631804		URO01284			
BO07793	FJ630933	UGO01329	URO01145	yes	yes	
BO12514	FJ632463	UGO01333	URO01180		yes	
BO07839	FJ630952	UGO01087			yes	
BO15495	FJ633496	UGO01210	URO01210	yes	yes	
BO12834	FJ632596	UGO01186	URO01343	yes	yes	
BO08189	FJ631094		URO01020			
BO16305	FJ633776	UGO01196	URO01196	yes	yes	
BO17804	FJ634221	UGO01283	URO01283	yes	yes	
BO08517	FJ631224	UGO01095	URO01095	yes	yes	
BO09558	FJ638669	UGO01155	URO01155	yes	yes	
BO17946	FJ634261	UGO01224			yes	
BO09057	FJ631370	UGO01246	URO01246	yes	yes	
BO04682	FJ629841	UGO01307	URO01035	yes	yes	
BO06220	FJ630306	UGO01055	URO01055	yes	yes	
BO06807	FJ630540		URO01317		yes	
BO12757	FJ632552	UGO01185			yes	
ND	~					
BO11037	FJ631967	UGO01254	URO01254		yes	
BO12007	FJ632279	UGO01176	URO01176	yes	yes	
BO04404	FJ629745	UGO01030	URO01030	yes	yes	
BO07171	FJ630695	UGO01069	URO01319	yes	yes	
BO08232	FJ631109	UGO01091	URO01091	yes	yes	

BO07547	FJ630835		URO01084		yes	
BO07291	FJ630738		URO01080		yes	
BO09261	FJ631453	UGO01321			yes	
BO12059	FJ632294	UGO01178			yes	
BO18480	FJ634433	UGO01227	URO01227	yes	yes	
BO09426	FJ631501		URO01117		yes	
BO13579	MN238605	UGO01269	URO01269	yes	yes	
BO08859	FJ631293		URO01238		yes	★
BO05869	FJ630177	UGO01046	URO01046	yes	yes	
BO13592	FJ632848	UGO01188	URO01188		yes	
BO10634	KX795535	UGO01290	URO01290	yes	yes	
BO06002	FJ630214	UGO01049	URO01049	yes	yes	
BO05874	FJ630181		URO01048		yes	
BO12754	FJ632550	UGO01184	URO01184	yes	yes	
BO16093	FJ633716	UGO01276			yes	
BO21842	KX793921	UGO01295	URO01295		yes	
BO12573	FJ632495	UGO01265	URO01265	yes	yes	
BO01335	FJ629477	UGO01013	URO01013	yes	yes	
BO06843	FJ630558	UGO01064	URO01318	yes	yes	
BO09719	FJ631556	UGO01118	URO01330	yes	yes	★
BO04710	FJ629849		URO01312		yes	
BO09202	FJ631427	UGO01107	URO01107	yes	yes	
BO17637	FJ634185		URO01233		yes	
BO05871	FJ630179	UGO01310	URO01047	yes	yes	
BO11934	FJ632250	UGO01172	URO01172	yes	yes	
BO10939	FJ631930		URO01334		yes	
BO14848	FJ633259	UGO01205	URO01205		yes	
BO09069	FJ631379	UGO01228	URO01228	yes	yes	
BO07139	FJ630682		URO01067			
BO09258	FJ631450	UGO01113	URO01113	yes	yes	
BO03884	FJ629591		URO01136		yes	
BO09010	FJ631350	UGO01319	URO01106	yes	yes	
BO07145	FJ630686	UGO01154	URO01154		yes	
BO13107	FJ632677	UGO01267	URO01267		yes	
BO10012	FJ631633		URO01121		yes	
BO16667	KX799925		URO01279		yes	
BO05402	FJ630015	UGO01140	URO01140	yes	yes	
BO05207	FJ629996	UGO01018	URO01308		yes	
BO14010	FJ632993	UGO01270	URO01270	yes	yes	
BO06051	FJ630254	UGO01052	URO01052	yes	yes	
BO02323	MN238601		URO01023		yes	

BO06064	FJ630265	UGO01053	URO01053		yes
BO09964	FJ631624	UGO01249	URO01249	yes	yes
BO03603	FJ629568	UGO01131	URO01335	yes	yes
BO10931	KX796096	UGO01291			
BO01347	FJ629482	UGO01014	URO01014		yes
BO11702	FJ632161	UGO01168	URO01168	yes	yes
BO15754	FJ633575	UGO01274			yes
BO18355	FJ634388	UGO01237	URO01237	yes	yes
BO11114	FJ632000	UGO01164			yes
BO11056	FJ631976	UGO01166	URO01166		yes
BO10477	FJ631783	UGO01126	URO01333	yes	yes
BO18165	FJ634336	UGO01225	URO01225	yes	yes
BO09294	FJ631466	UGO01323	URO01116		yes
BO10346	FJ631714	UGO01122	URO01122	yes	yes
BO15737	FJ633566	UGO01213	URO01213	yes	yes
BO09318	FJ631471	UGO01153	URO01153	yes	yes
BO07339	FJ630755		URO01322		
BO11882	FJ632233		URO01341		yes
BO06740	FJ630512	UGO01059	URO01059	yes	yes
BO01082	FJ629415	UGO01004	URO01004	yes	yes
BO11972	FJ632264	UGO01173	URO01340	yes	yes
BO01534	FJ629531	UGO01008			yes
BO09644	FJ631548	UGO01024	URO01024		yes
BO16578	FJ633869	UGO01232	URO01232		yes
BO08805	FJ631277	UGO01149	URO01149	yes	yes
BO08205	FJ631097	UGO01090	URO01090	yes	yes
BO04754	FJ629859	UGO01038	URO01038	yes	yes
BO07259	FJ630725	UGO01076	URO01076		yes
BO10607	FJ631812	UGO01251	URO01251		yes
BO12711	FJ632528	UGO01183	URO01183	yes	yes
BO04026	FJ629603		URO01027		yes
BO16091	FJ633715	UGO01275	URO01275	yes	yes
BO11255	FJ632044	UGO01259	URO01259	yes	yes
BO06401	FJ630377	UGO01056	URO01316	yes	yes
BO06837	FJ630554		URO01063		yes
BO05420	FJ630026	UGO01043			yes
BO11216	KX793935	UGO01256			yes
BO11243	FJ632038	UGO01257	URO01257	yes	yes
BO07395	FJ630772	UGO01081			yes
BO11956	FJ632257	UGO01261	URO01261	yes	yes
BO16764	FJ633905	UGO01280	URO01280		yes

BO09207	FJ631429	UGO01320	URO01108	yes	yes
BO04294	FJ629722	UGO01305			yes
BO08991	FJ631342	UGO01105	URO01105		yes